



Hippocampal neurogenesis promotes preference for future rewards

Désirée R. Seib¹ · Delane F. Espinueva¹ · Oren Princz-Lebel¹ · Erin Chahley¹ · Jordann Stevenson¹ · Timothy P. O'Leary¹ · Stan B. Floresco¹ · Jason S. Snyder¹

Received: 19 January 2021 / Revised: 29 April 2021 / Accepted: 6 May 2021
© The Author(s), under exclusive licence to Springer Nature Limited 2021

Abstract

Adult hippocampal neurogenesis has been implicated in a number of disorders where reward processing is disrupted but whether new neurons regulate specific aspects of reward-related decision making remains unclear. Given the role of the hippocampus in future-oriented cognition, here we tested whether adult neurogenesis regulates preference for future, advantageous rewards in a delay discounting paradigm for rats. Indeed, blocking neurogenesis caused a profound aversion for delayed rewards, and biased choice behavior toward immediately available, but smaller, rewards. Consistent with a role for the ventral hippocampus in impulsive decision making and future-thinking, neurogenesis-deficient animals displayed reduced activity in the ventral hippocampus. In intact animals, delay-based decision making restructured dendrites and spines in adult-born neurons and specifically activated adult-born neurons in the ventral dentate gyrus, relative to dorsal activation in rats that chose between immediately-available rewards. Putative developmentally-born cells, located in the superficial granule cell layer, did not display task-specific activity. These findings identify a novel and specific role for neurogenesis in decisions about future rewards, thereby implicating newborn neurons in disorders where short-sighted gains are preferred at the expense of long-term health.

Introduction

Adult hippocampal neurogenesis is implicated in a wide range of psychiatric disorders that are not traditionally viewed as disorders of memory, raising questions about their role in other aspects of cognition and mental health [1]. This question has been difficult to address from a disease perspective, given the complexity of psychiatric disorders that cannot be perfectly modeled in animals. One fruitful approach may be to investigate whether adult-born neurons are involved in specific behavioral processes that are disrupted in human disorders [2]. Given that human psychiatric disorders are often overlapping, this approach may also help identify how neurogenesis contributes to such a diverse range of disorders.

Reward-related behaviors are commonly disrupted in neuropsychiatric disorders but, to date, few studies have investigated a possible role for neurogenesis. Blocking neurogenesis promotes drug-seeking behavior in animal models of cocaine [3, 4] and methamphetamine [5] addiction. However, neurogenesis is often dispensable for behaviors related to natural rewards. In the standard version of the sucrose preference test, where water and sucrose are freely available in fixed locations, neurogenesis minimally contributes to reward consumption, if at all [6–11]. In operant paradigms, neurogenesis-deficient animals also often show normal reward learning and reward sensitivity [3, 5, 12]. However, patient populations may be able to experience rewards normally, but exhibit deficits in motivation and decision-making that impair their ability to obtain them [13]. Indeed, disrupting neurogenesis *does* reduce sucrose preference when the location of water and sucrose unexpectedly switch locations [6, 8], suggesting new neurons may regulate cognitive aspects of reward seeking. Recent work also indicates that neurogenesis increases motivation to obtain natural rewards [12] and facilitates learning about uncertain rewards [14]. Whether neurogenesis contributes to other aspects of reward behavior, particularly those related to cost-benefit decision making, remains unclear.

Supplementary information The online version contains supplementary material available at <https://doi.org/10.1038/s41380-021-01165-3>.

✉ Jason S. Snyder
jasonsnyder@psych.ubc.ca

¹ Department of Psychology, Djavad Mowafaghian Centre for Brain Health, University of British Columbia, Vancouver, BC, Canada

Delay discounting is one aspect of reward processing that features prominently in a number of psychiatric disorders [15, 16]. Here, subjects place less value on future rewards, which shifts choice away from larger/preferred, but delayed, outcomes. While reward-based decision making is typically considered the domain of frontal and striatal regions [17, 18], the hippocampus is particularly well suited for guiding choices related to future experiences: hippocampal activity patterns reflect future-oriented behaviors in both rodents [19–22] and humans [23, 24], amnesics have an impoverished imagination of scenes [25] and possible future events [26], and hippocampal damage biases humans [27, 28] and animals [29–31] toward immediately-available rewards, at the expense of larger, delayed, rewards. We therefore hypothesized that adult neurogenesis may be specifically involved in decisions about future rewards. To examine this, we tested neurogenesis-deficient rats in a nonspatial delay discounting task and measured activity and plasticity in newborn hippocampal neurons as rats chose between small, immediately-available rewards and larger, delayed rewards. Consistent with our hypothesis, blocking neurogenesis caused a profound aversion for delayed rewards and delay-based decision making specifically activated and induced plasticity in newborn neurons.

Methods

Animals

All procedures were approved by the Animal Care Committee at the University of British Columbia (UBC) and conducted in accordance with the Canadian Council on Animal Care guidelines regarding humane and ethical treatment of animals. Sample sizes were based on experience from previous work where moderate effects were detected ($n = 10$ – 16 /group for behavioral experiments, $n = 8$ /group for immediate-early gene cell counts). For all experiments, animals were randomly assigned to treatments and behavioral conditions, and the experimenter was blinded to the treatment conditions during testing, data acquisition and data analysis. Experimental male Long-Evans rats were generated from breeders ordered from Charles River, Canada. Transgenic male rats expressing HSV-TK (TK; also on a Long-Evans background) under the human GFAP promoter were generated by breeding transgenic female rats with nontransgenic male rats that were ordered from Charles River, Canada. All breeding and most testing occurred in the Department of Psychology animal facility with a 12-hour light/dark schedule and lights on at 9:00 am. The exception is the data presented in Fig. 6, which was obtained using male Long-Evans rats that were ordered from Charles River, Canada, and tested in the UBC Center for Disease Modeling animal facility.

Experiments were performed during the light phase of the light/dark cycle. Breeding occurred in large polyurethane cages ($47 \times 37 \times 21$ cm) for TK rats, and in Opti-rat cages for the Long-Evans rats that were tested in the irradiation and running experiment. Cages contained a plastic tube, aspen chip bedding and ad libitum rat chow and water. Breeders (both male and female) remained with the litters until P21, when offspring were weaned to 2 per cage in smaller polyurethane bins ($48 \times 27 \times 20$ cm) and transgenic rats were genotyped afterwards.

TK rat model

In transgenic GFAP-TK rats neurogenesis was suppressed by manually giving 4 mg valganciclovir to each rat in a single 0.5 g pellet of 50% chow and 50% peanut butter twice per week for 6 weeks starting at 6 weeks of age, as we have done before [7, 32, 33]. 12-week-old male TK and WT littermates were used for behavioral testing, lasting ~5 weeks, at which point rats were perfused for histology. Animals were single housed and food restricted at 11 weeks of age, over the course of one week, to 90% of their initial weight at the start of each experiment. Animals were handled prior to operant training for a minimum of 5 min for 5 days by the experimenters. Our first experiment, where WT and TK rats were given valganciclovir and tested on the delay discounting task (Fig. 1E), was comprised of a total of 14 WT rats and 16 TK rats. This reflected 2 different batches of animals that were tested at separated times. One batch was subjected to acute restraint stress prior to the final day of behavioral testing (7 WT rats, 11 TK rats; Fig. 1F) and the other batch was used to assess task-related immediate-early gene expression on the final day of behavioral testing (7 WT rats, 5 TK rats; Fig. 3).

Irradiation

We used irradiation as an alternative model to deplete neurogenesis [34]. Six-week-old male Long-Evans rats were irradiated (IR) on 2 consecutive days with 5 Gray per day, resulting in a total dose of 10 Gray ($n = 10$). Rats were anesthetized with 50 mg/kg and 60 mg/kg sodium pentobarbital on the first and second day, respectively. We used a RadSource RS 2000 irradiator from RadSources Technologies, Inc., Suwanee, USA. Up to 4 animals' hippocampi were simultaneously irradiated while their bodies were shielded with 3 mm lead except a window above the hippocampus. Sham irradiated ($n = 10$) rats received anesthesia only. Side effects that were caused by irradiation: Gray hair appeared from 2 weeks after IR. Some animals developed a scab at the irradiation site. All 10 animals had to get their teeth trimmed, 2 animals received 1 mg/kg Anafen, three

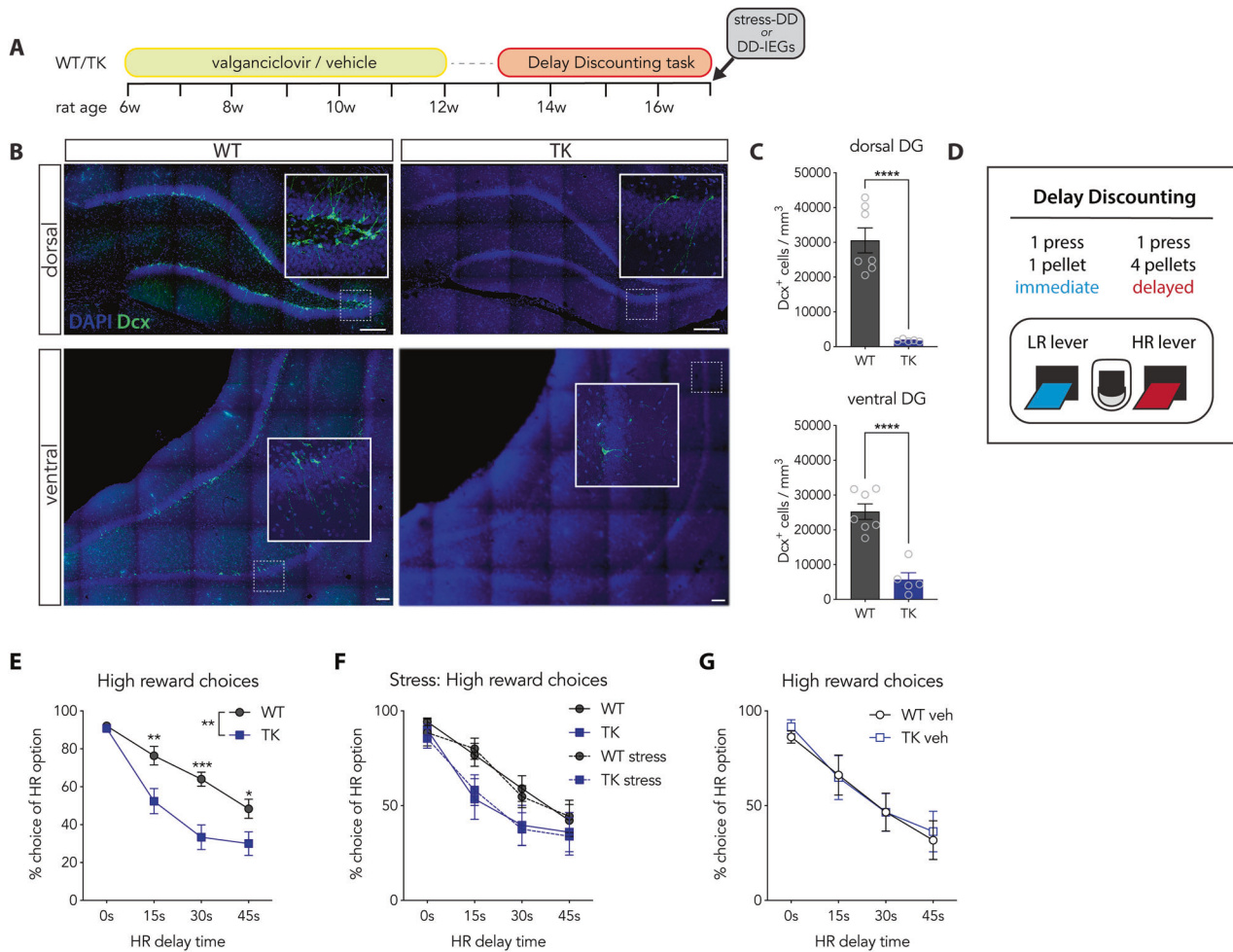


Fig. 1 Neurogenesis promotes preference for delayed rewards. **A** Experimental timeline for testing delay discounting behavior in valganciclovir- and vehicle-treated WT and TK rats. WT and TK littermates were treated with valganciclovir to block neurogenesis and were then trained in the DD task. On the final day, one cohort of animals were subjected to acute stress prior to DD testing. The other cohort was tested on the DD task and brains were collected to assess task-related IEG activation (see Fig. 3, Supplementary Fig. 4). **B** Immunostaining for the immature neuron marker Dcx in the dorsal and ventral hippocampus of WT and TK rats. Scale bars, 200 μ m. **C** Neurogenesis was reduced in the dorsal and in the ventral DG in valganciclovir-treated TK rats (dorsal, $T_{10} = 6.7$, $P < 0.0001$; ventral, $T_{10} = 6.3$, $P < 0.0001$, $n = 5-7$ /group). **D** Overview of the DD operant task. **E** TK rats, which lacked adult neurogenesis, preferred the high

reward less when a delay was imposed (RM ANOVA: effect of genotype, $F_{1,28} = 9.8$, $P = 0.0040$; effect of delay, $F_{3,84} = 99$, $P < 0.0001$; interaction, $F_{3,84} = 7.4$, $P = 0.0002$; post-hoc Holm Sidak tests: WT vs. TK at 15 s, $P = 0.004$; WT vs. TK at 30 s, $P = 0.0002$; WT vs. TK at 45 s, $P = 0.04$; $n = 14-16$ /group). **F** Restraint stress did not alter WT or TK behavior in the DD task compared to the previous, unstressed, day of testing (treatment x time RM ANOVA: WT effect of stress $F_{1,6} = 0.13$, $P = 0.73$; TK effect of stress $F_{1,10} = 0.1$, $P = 0.8$). **G** Delayed reward preferences were not different between vehicle-treated WT and TK rats (genotype x time RM ANOVA: effect of genotype, $F_{1,14} = 0.036$, $P = 0.85$; effect of time, $F_{3,42} = 40$, $P < 0.0001$; interaction, $F_{3,42} = 0.2$, $P = 0.9$). Graphs display mean \pm standard error. LR, low reward; HR, high reward; s, seconds; w, weeks. * $P < 0.05$; ** $P < 0.01$; *** $P < 0.001$, **** $P < 0.0001$.

times. All animals received a single dose of 200 mg/kg 5-bromo-2'-deoxyuridine (BrdU) to label dividing neural progenitor cells in order to determine effectiveness of IR at 9 weeks of age, 3 weeks after IR. Histology for BrdU and Dcx was performed at the end of the experiment.

Retrovirus production

The retroviral vector used in this study was derived from a Moloney Murine Leukemia-Virus (MMLV), in which

eGFP expression is driven by a Ubiquitin (Ubi) promoter. Retroviral Ubi-eGFP (MMLV-eGFP; kindly provided by Dr. Shaoyu Ge) and VSV-G (kindly provided by Dr. Ana Martin-Villalba) plasmids were transfected in HEK293-GP cells (kindly provided by Dr. Diane Lagace) using PEI. Retrovirus was harvested 2 and 3 days after transfection, followed by ultracentrifugation (2 h at 27,000 rpm). Retroviruses were produced as described previously [35]. Viral titers ranged from 1 to 8×10^6 colony forming units/ml.

Stereotaxic surgery and behavioral testing

Rats were bred in house and were handled for 5 days the week before surgery for 3 min per day. At 6 ($n = 13$) or 10 ($n = 5$) weeks of age rats were anesthetized using isoflurane and oxygen and injected bilaterally in the dorsal (anteroposterior = -4.0 mm; mediolateral = ± 3.0 mm; dorsoventral = -3.5 mm from skull) and ventral (anteroposterior = -6.0 mm; mediolateral = ± 4.7 mm; dorsoventral = -6.5 mm from skull) hippocampus using standard stereotaxic techniques. Bregma was measured at the top of the skull. In total, 1 μ l of virus suspension was injected at each site at 200 nl/min. Local injection of Bupivacaine (8 mg/kg) was used as analgesic prior to surgery. Anafen (5 mg/kg) was given once a day for 3 days starting just before the surgery. Animals had at least 5 days to recover after the surgery before being food deprived for behavioral testing. Rats were food deprived at 11 weeks of age and operant training started at 12 weeks of age. Training on the No Delay (ND) and Delay Discounting (DD) tasks was performed for 4 weeks after ~ 10 days of initial operant training. Brain tissue was collected 35 min after animals finished operant testing on the last day of training.

Activation of BrdU⁺ adult-born neurons

A single batch of 5- and 9-week-old male rats were ordered from Charles River. At 6 and 10 weeks, respectively, rats were injected with 200 mg/kg BrdU daily for 5 consecutive days to label newly generated neurons. These rats were then trained in operant chambers and run on the No Delay (ND) and Delay Discounting (DD) tasks starting at 12-weeks of age (tasks described below). Neurons that were labeled with BrdU at 6 weeks of rat age were 7 weeks old when animals started the ND/DD tasks, and 11 weeks old when brains were collected for histological analyses; we refer to these neurons as “mature neurons”. Neurons that were labeled with BrdU at 10 weeks of rat age were 3 weeks old when animals started the ND/DD tasks, and 7 weeks old when brains were collected for histological analyses; we refer to these neurons as “immature neurons”. Animals were sacrificed 35 min after ending the ND/DD tasks on the last day of the experiment (90 min after the start of the experiment) and were then immunostained for immediate-early gene markers of neuronal activity (Zif268, Fos, Arc). One rat from the “immature” DD group was excluded due to tumor-like growth in the dorsal dentate gyrus. One rat from the “mature” ND group had poor BrdU/Zif268 immunostaining and was not analyzed. Thus, the total number of animals/group for this experiment was: No Delay mature neurons ($n = 8$), No Delay immature neurons ($n = 8$, except $n = 7$ for Zif268), Delay Discounting immature neurons ($n = 7$), Delay Discounting mature neurons ($n = 8$).

Behavior

All animal testing was conducted in 24 operant chambers (30.5 cm \times 24 cm \times 21 cm; Med Associates, St Albans, VT, USA) enclosed in sound-attenuating boxes as described before [14]. Each box was equipped with a fan to provide ventilation and mask external noise. The chambers were equipped with two retractable levers on either side of a central food receptacle where food reinforcement (45 mg sugar pellet; Bioserv, Frenchtown, NJ, USA) was delivered by a pellet dispenser. The chambers were illuminated by a 100 mA house light located on the top center of the wall opposite the levers. Four infrared photocell sensors were positioned on the walls adjacent to the levers. Locomotor activity was indexed by the number of photo beam breaks that occurred during a session. The food receptacle contained an infrared head entry detector to determine the number of nosepokes. All experimental data were recorded by personal computers connected to chambers through an interface.

Pretraining

On the day before their first exposure to the operant chambers, each animal received ~ 25 reward pellets in their home cage. On the first day of training, rats were in the operant chamber for 30 min and 1 reward pellet was delivered into the food receptacle every 30 s. On the second day of training, the food receptacle contained 2–3 reward pellets and crushed pellets were placed on the extended lever before each rat was placed in the chamber. First, rats were trained to press one of the levers to receive a reward on a fixed-ratio 1 (FR1) schedule to a criterion of 60 presses in 30 min. Levers were counterbalanced left/right between subjects. When the criterion was met, FR1 training was conducted on the other lever to ensure that both levers were experienced.

Rats were then run on 90-trial sessions that started with the levers retracted. Every 30 s, a new trial was initiated by the extension of one of the two levers into the chamber. If the rat failed to respond to the lever within 10 s, the lever was retracted, the house light was extinguished and the trial was scored as an omission. A response within 10 s of lever insertion resulted in delivery of a single pellet. In every pair of trials, the left or right lever was presented once, and the order within the pair of trials was random. Rats were trained for 3–5 days on this task to a criterion of 80 or more successful trials (i.e., ≤ 10 omissions).

No delay (ND) task

The ND task is identical to the DD task that the animals were ultimately trained on, except that the low (1 pellet) and

the high rewards (4 pellets) were both delivered immediately after 1 lever press. Animals were trained on the ND task for 2 consecutive days before the DD task. The high reward was counterbalanced between the left and right levers across animals. Each day, animals received one training session with 4 blocks of 12 trials. Each block consisted of 2 forced choice trials (only one lever extends) and 10 free choice trials (both levers extend). Every 70 s the house light came on and one or both levers extended. If the rat did not press a lever during the next 10 s, the levers retracted and the trial was counted as an omission. Animals merely had to choose between a low and a high reward and thus quickly learned to prefer the high reward over the low reward. Thus, animals in the TK and IR experiments, that ultimately went on to perform the DD task, had only 2 days of ND testing and analyses focussed on the 2nd day of this task. ND animals in the BrdU-IEG and retrovirus experiments continued to be trained on this task for 28 days.

Delay discounting (DD) task

After 2 days of the ND task, animals received daily training sessions on the DD task. Like in the ND task, one session consisted of 48 trials, divided into 4 blocks. The lever (left or right, counterbalanced across animals) that was assigned to the high reward (HR) in the ND task remained associated with the HR in the DD task. One block started with 2 forced choice trials, where only one of the reward levers was extended (one trial for each lever, presented randomly), followed by 10 free choice trials. The inter-trial interval (ITI) was 70 s, regardless of lever choice, leading to a total of 56 min per session. At the beginning of each choice trial, the house light was illuminated and both levers extended after 2 s. If the rat failed to respond within 10 s, similar to the lever-press training, both levers would retract, the trial would be scored as an omission, and houselights would go off until the next trial began. On each choice trial, a press on the low reward (LR) lever retracted both levers and delivered one sugar pellet immediately. Choice of the HR lever also retracted both levers immediately, but 4 pellets were delivered after a delay, which increased over the 4 blocks of trials (0 s, 15 s, 30 s, 45 s). During the delay, the chamber remained in darkness as in the ITI and was re-illuminated during the reward delivery at the end of the delay. Pellets were delivered 0.5 s apart. After the delivery of the reward, the house light remained lit for another 4 s before it returned to ITI state. Daily training sessions continued for 7 days a week until behavioral performance was judged to be stable when there was $\leq 15\%$ variation for 3 straight days, which occurred after 28–31 days of testing in the experiments from this study. When quantifying IEG expression or morphology of virally labeled neurons, animals were perfused and brains were collected 35 min after the final

DD session. Half of the animals from the main TK DD experiment (behavior data presented in Fig. 1E) were used for IEG analyses (presented in Fig. 3). The other half were used to study the effects of acute restraint stress on DD behavior (Fig. 1F).

Restraint stress

Acute stress was induced by restraining rats for 30 min in a plexiglas cylindrical restrainer tube (Broome style rodent restrainer 250 g to 500 g; 6.35 cm \times 6.35 mm \times 21.6 cm; Plas Labs, Inc.) in a quiet, lit and ventilated room. After rats were placed in the tubes, restrainer length was adjusted to keep rats immobilized without causing pain. Upon being released from the tube into their home cage, rats were immediately transported to the operant chamber to start the DD task. Corticosterone was not measured in stressed, DD-tested rats to avoid possible confounding effects of blood sampling. To verify that restraint induced a stress response, a separate group of nontransgenic male Long Evans rats was subjected to restraint ($n = 5$) in the same fashion and blood was collected immediately after restraint and corticosterone levels were determined by radioimmunoassay. Transport control ($n = 4$) rats were similarly brought out to the testing area but were not handled or restrained prior to blood sampling.

Immunofluorescence

Animals were anesthetized using isoflurane and transcardially perfused with 4% paraformaldehyde (PFA) in PBS. Brains were extracted and post-fixed for 48 h in 4% PFA. To analyze IEG activity or assess levels of neurogenesis, tissue was cut at 50 μm on a vibratome. To examine neuronal morphology of virally labeled new-born neurons, tissue was cut at 100 μm on a vibratome. Cut tissue was stored in anti-freeze at -20°C until further processing.

Free floating sections were washed three times in PBS. When staining for BrdU, we additionally incubated sections in 2 N HCl for 30 min at RT and washed tissue 5 times in PBS for 3 min [36]. For Fos immunostaining, Fos immunohistochemistry and amplification was conducted prior to detection of other antigens: First, sections were incubated with 1% hydrogen peroxide to inactivate endogenous peroxidase activity, followed by one 5 min PBS wash at RT. Then, sections were incubated in blocking solution (3% horse serum and 0.5% Triton-X) and incubated with primary goat anti-cfos (Santa Cruz, sc-52, 1:200) antibody at 4°C for 72 h. Sections were washed three times and then incubated with the biotinylated donkey anti-goat secondary antibody (Jackson Immunoresearch Labs, 705-065-147, 1:250) in blocking solution for 2 h at 4°C . After 3 washes, sections were incubated in 5% blocking solution (Perkin

Elmer, FP1020) for 30 min at RT. Subsequently, sections were incubated with Streptavidin-HRP (Perkin Elmer, NEL750001EA, 1:100) for 1 h at RT in 5% blocking solution. After three PBS washes, sections were incubated in NHS-Rhodamine (Fisher, PI-46406, 1:2000 in PBS with 1:20,000 33% H₂O₂) for 30 min at RT. Sections were washed three times with PBS before other stainings followed.

For all immunohistochemistry, sections were incubated in blocking solution (3% horse serum and 0.5% Triton-X). The following primary antibodies were used: mouse anti-GFP (DSHB, GFP-12E6, 1:100), rabbit anti-Zif268 (Santa Cruz, sc189, egr-1, 1:1000), goat anti-Dcx (Santa Cruz, C-18, 1:200), goat anti-TK (Santa Cruz, sc28038, 1:200), mouse anti-BrdU (BD Biosciences, 347580, 1:200), and rabbit anti-Arc (Synaptic Systems, 156003, 1:1000). Sections were incubated in primary antibodies at 4 °C for 72 h. Sections were washed three times and then incubated with secondary antibodies (1:400, Invitrogen) in blocking solution for 2 h at 4 °C (donkey anti-mouse Alexa488, donkey anti-goat Alexa555, donkey anti rabbit Alexa647). Sections were then washed three times, nuclei were stained with DAPI (1 mg/ml, diluted 1:1000 in PBS) for 5 min, washed three times in PBS and then mounted on glass cover slides and cover slipped with PVA-Dabco to preserve fluorescence.

BrdU and Dcx cell counting

Images of the dorsal and ventral dentate gyrus were taken using a water-immersion 25x objective (N.A. 0.95) on a Leica SP8 confocal microscope. Images were 1024 × 1024 pixels in size, taken at 1x zoom, a speed of 200 Hz, with a z-height of 1 μm. Analysis of Dcx and BrdU positive cells in the GCL layer of the dorsal and ventral hippocampal DG were performed manually using ImageJ [37] and the Cell Counter Plugin. Cell densities were calculated by dividing the number of positive cells in the GCL of the DG by the GCL volume. Dorsal images were taken at $-3.5 \text{ mm} \pm 0.6 \text{ mm}$ Bregma and ventral images were taken at $-6.0 \text{ mm} \pm 0.4 \text{ mm}$ Bregma.

Dendrite analyses

Images of dendritic trees in the dorsal and ventral dentate gyrus were taken using a water-immersion 25x objective (N.A. 0.95) on a Leica SP8 confocal microscope. Images were 1024 × 1024 pixels in size, taken at 1x zoom, a speed of 200 Hz, with a z-height of 1 μm. Simple Neurite Tracer [38] was used to trace dendritic trees of newborn granule cells to collect data for Sholl analysis, branching and total dendritic length. Sholl analyses were restricted to 0–300 μm since dendrites did not reliably extend beyond this range.

Branch points were manually counted from the traces by the experimenter. Five neurons from the suprapyramidal blade were recorded per GFP positive animal in the dorsal and ventral hippocampus. Neurons with more than 3 primary and secondary dendrites cut due to tissue processing were excluded from the analysis [39].

Spine analyses

Images of spines were taken using a glycerol-immersion 63x objective (N.A. 1.3) on a Leica SP8 confocal microscope. Images were 1024 × 1024 pixels in size, taken at 5x zoom, a speed of 100 Hz, with line averaging (2x) and a z-height of 1 μm. Five dendrite segments of ~40 μm length, from different neurons in the suprapyramidal blade, were recorded per GFP positive animal in the dorsal and ventral hippocampus. Dendrite length was measured using Simple Neurite Tracer. Spines were counted manually by a human experimenter blind to the experimental conditions using the Cell Counter plugin in ImageJ. Mushroom spines were measured with ImageJ and defined as having a diameter $\geq 0.6 \mu\text{m}$.

Analyses of neuronal activity with immediate-early genes (IEG)

Images of the hippocampal DG suprapyramidal blade and CA3a,b,c subregions were taken using a water-immersion 25x objective (N.A. 0.95) on a Leica SP8 confocal microscope. Images were 1024 × 1024 pixels in size, taken at 1x zoom, a speed of 200 Hz, with a z-height of 1 μm. Cells expressing Zif268, Fos and Arc were counted with the ImageJ Cell Counter plugin. In the DG, due to the graded nature of Zif268 expression and large number of weakly-positive cells, only strongly positive cells were counted (4x brighter than background staining in the molecular layer). In CA3, where Zif268 expression was generally weaker, cells expressing at 2x background levels were counted as positive. Due to the high number of Zif268-positive cells in CA3, analyses were limited to 2 Z-planes within a stack ($\geq 7 \mu\text{m}$ apart) and, thus, positive cells are expressed per area rather than per 3D volume. Fos and Arc positive cells were very distinct, less frequent than Zif268-positive cells and were therefore counted manually (i.e., without measuring intensities) throughout the full slice thickness. Consistent with previous reports [40], somatic Arc immunostaining was not sufficiently bright in CA3 and therefore Arc was not quantified in this region. Cell densities in the DG and CA3 were calculated dividing the number of positive cells by the respective volume of the cell body layer. In dorsal sections, CA3a was defined as the curved portion of CA3 that bordered CA2/CA1, CA3c was defined as the portion of CA3 that was enclosed by the blades of the DG, and

CA3b was the relatively linear portion in between CA3a and CA3c.

To assess IEG expression in immature and mature BrdU-labeled granule neurons, images of the suprapyramidal blade of the dorsal and ventral dentate gyrus were taken using a water-immersion 25x objective (N.A. 0.95) on a Leica SP8 confocal microscope. Images were 1024 × 1024 pixels in size, taken at 1x zoom, a speed of 400 Hz, with a z-height of 1.5 μm. Approximately 100 BrdU-positive cells were analyzed in each area (dorsal and ventral) for each animal. BrdU cells that were strongly positive for Zif268 were counted (4x brighter Zif staining in BrdU cells than background staining in the molecular layer). BrdU cells positive for Fos and Arc were very distinct and counted manually without measuring intensities. To estimate activity rates in putative developmentally-born neurons, we analyzed IEG expression in DAPI⁺ cells that were located in the superficial half of the granule cell layer, since birth-dating studies have found that these cells are overwhelmingly generated during the fetal and perinatal periods [41, 42]. IEG activity in this population was measured in the same tissue used for BrdU-IEG analyses. We analyzed 8 rats from each of the DD and ND groups, half of which were injected with BrdU for the immature neuron analyses and the other half for the mature neuron analyses. At least 100 DAPI⁺ cells were analyzed for Zif268 and at least 200 DAPI⁺ cells were analyzed for Fos and Arc (per dorsal and ventral subregion). Activity rates are expressed as the percentage BrdU⁺ or DAPI⁺ cells that were also positive for IEGs.

Statistical analyses

Unpaired, two-sided *t* tests and one- or two-way ANOVAs were used to analyze effects of genotypes and treatments on neurogenesis, IEG expression, neuronal morphology and behavior, as indicated. When we observed significant interactions, we used Holm Sidak post hoc tests to compare groups. In cases where data were not normally distributed, data were analyzed by non-parametric Mann–Whitney test, or Kruskal Wallis test followed by post hoc Dunn's test. In the majority of experiments there was equal variance between groups that were compared. The only exceptions were cases where different variances reflected intended experimental manipulations and expected group differences: those that compared newborn neurons in intact animals to animals that lacked neurogenesis (TK, IR), and cases where immediate-early gene-expressing cells were observed in one group/region but were (nearly) absent in another. In all cases, statistical significance was set at $P = 0.05$. Statistical analyses can be found in the main text for data that are not presented in the figures. For data that are presented in the figures, statistical analyses can be found in the figure legends.

Results

Blocking neurogenesis reduces preference for delayed rewards

Delayed rewards typically have less subjective value than immediately-available rewards, a phenomenon known as delay discounting (DD) [15]. To determine whether adult neurogenesis promotes the choice of future rewards, we used the transgenic GFAP-TK rat model to deplete neurogenesis [7] and a DD decision-making task that has been optimized for rats [43] (timeline in Fig. 1A). As measured by the immature neuronal marker, DCX, neurogenesis was reduced in valganciclovir-treated TK rats by 94% in the dorsal DG and 77% in the ventral DG, compared to valganciclovir-treated wild type (WT) littermates (Fig. 1B, C; hereafter, “WT” and “TK” refers to valganciclovir-treated animals, and “WT veh” and “TK veh” refers to vehicle-treated animals in control experiments). Blockade of neurogenesis reduced the overall volume of the dentate granule cell layer (Supplementary Fig. 1A), consistent with previous reports of a smaller DG in TK rats [10]. DG atrophy also mirrors the smaller DG/hippocampal volume that is observed in a number of psychiatric disorders that are characterized by increased delay discounting including depression [44, 45] schizophrenia [44] and aging/Alzheimer's disease [45, 46]. Neurogenesis was not noticeably reduced in the subventricular zone, likely due to faster recovery in this neurogenic region during the valganciclovir-free period of operant testing (Supplementary Fig. 1B–C).

Intact WT and neurogenesis-deficient TK rats were then tested on the DD paradigm, where they were given a choice between a small reward (1 sugar pellet) that was delivered immediately and a high reward (4 pellets) that was delivered after a delay (Fig. 1D). Male rats received 1 session per day for 4 weeks, where each session consisted of 4 blocks of 10 trials. Over the 4 blocks the delay to receive the high reward increased from 0 s to 15 s, 30 s and 45 s. During pretraining, when rewards were presented without a delay (No Delay task, ND), both WT and TK rats showed a clear preference (>85%) for the high reward (Supplementary Fig. 2B). In the DD task, choice of the high reward decreased with longer delay periods, as expected (Fig. 1E). However, with increasing delays, neurogenesis-deficient TK rats chose the high reward significantly less than WT rats. The delay discounting phenotype in TK rats was not due to reduced motivation to perform the task, since trial omissions and choice latencies were comparable to intact WT rats. TK rats also displayed normal levels of locomotion and nosepoke behavior suggesting that task performance was not confounded by non-specific motor deficits (Supplementary Fig. 2C–G).

Adult neurogenesis regulates the behavioral responses to stress [6, 47, 48] but it is not known if decision-making is impacted by stress in a neurogenesis-dependent fashion. We therefore subjected ~half of the WT and TK rats to 30 min restraint stress prior to the final session of DD testing. In a separate group of non-transgenic rats that were not tested on the DD task, restraint caused a ~6x elevation in corticosterone, thereby validating the stressor (Supplementary Fig. 2H). However, in both WT and TK rats, behavioral performance was similar to unstressed conditions from the previous day (Fig. 1F). These data are consistent with evidence that DD behavior is not impacted by acute stress [49] and they indicate that neurogenesis depletion does not amplify any latent effects of stress on delayed reward preferences.

To confirm the specificity of the TK model we performed two additional control experiments. First, we tested vehicle-treated WT and TK rats that did not receive valganciclovir, and therefore had intact neurogenesis. Here, both genotypes displayed equivalent rates of discounting (Fig. 1G) and were comparable in all other behavioral measures (Supplementary Fig. 2M–R), indicating that the delay discounting behavior in TK rats is due to loss of neurogenesis and not off-target effects of the transgenic line. Second, we subjected non-transgenic rats to irradiation to determine whether we could replicate the DD phenotype with an independent method for inhibiting neurogenesis (Fig. 2). Compared to sham-irradiated controls, irradiated rats had a complete loss of neurogenesis and they displayed greater

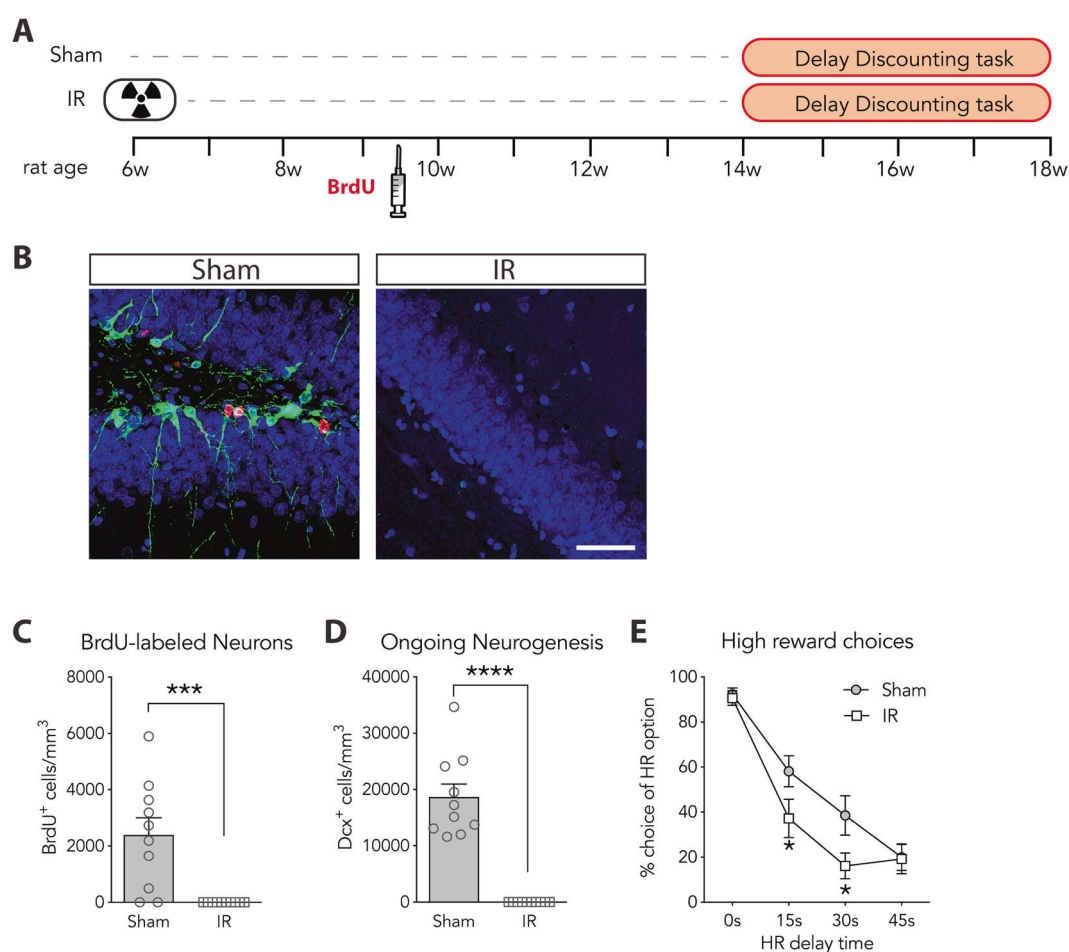


Fig. 2 Effects of irradiation and running on neurogenesis and delay discounting. **A** Experimental timeline for testing DD behavior in irradiated (neurogenesis-deficient; IR) and sham-irradiated rats. **B** Images of BrdU-labeled neurons (red) and Dcx⁺ immature neurons (green) in sham and IR animals. Scale bar, 50 μ m. **C** Irradiation greatly-reduced the number of BrdU⁺ cells (Mann–Whitney test, $P = 0.0007$; $n = 10$ /group). **D** Ongoing neurogenesis, during the last few weeks of the experiment, was assessed by counting immature Dcx⁺ cells. Dcx⁺ cells remained low in IR rats compared to sham rats

(Mann–Whitney test, $P < 0.0001$; $n = 10$ /group). **E** Irradiation reduced preference for the high reward in the DD task (group \times delay RM ANOVA: effect of group, $F_{1,18} = 2.3$, $P = 0.14$; effect of delay: $F_{3,54} = 126$, $P < 0.0001$; interaction: $F_{3,54} = 4.2$, $P = 0.009$; post-hoc Holm Sidak tests: sham vs. IR at 15 s, $P = 0.022$; sham vs. IR at 30 s, $P = 0.015$; $n = 10$ /group). Behavior graphs display the mean \pm standard error for the last 3 test days. LR, low reward; HR, high reward; s, seconds; w, weeks. * $P < 0.05$; *** $P < 0.001$; **** $P < 0.0001$.

DD behavior. Irradiated rats were otherwise similar to cage controls except they were slower to make a choice in the DD task (Supplementary Fig. 3), which is likely not due to reduced neurogenesis since we did not observe this behavior in TK rats.

Neurogenesis promotes activity in the ventral hippocampus during delayed reward choice

To determine whether blocking neurogenesis leads to abnormal patterns of activity that may underlie the reduced preference for delayed rewards, we quantified activity-dependent immediate-early gene (IEG) expression in a cohort of WT and TK rats after they completed the final session of DD testing (the cohort that did not undergo restraint stress on the final day of testing). A separate group of untested, non-transgenic cage controls was included to assess baseline levels of IEG expression. We examined both the dorsal and ventral subregions of the DG, since the ventral hippocampus has been specifically implicated in delayed reward choice [31]. Both WT and TK rats had increased Zif268 expression in the dorsal DG after performing the DD task compared to controls (Fig. 3A,B). In contrast, whereas there was a robust increase in Zif268 expression in the ventral DG of WT rats, activation was severely blunted in TK rats. Neurogenesis-dependent differences in neuronal recruitment extended to downstream region CA3, where TK rats had significantly fewer activated neurons in ventral CA3 than WT rats (Fig. 3C). Activity in dorsal CA3 was not globally affected by reduced neurogenesis but, when analyzed by subregion, CA3c showed less activity in TK rats (Fig. 3D). To examine the generality of these results we also examined expression of the IEGs Fos and Arc. Whereas Zif268 tended to show similar (DG) or greater (CA3) DD-induced expression in the ventral hippocampus, these IEGs showed greater (DG Fos, CA3 Fos) or exclusive (DG Arc) experience-dependent expression in the *dorsal* hippocampus, indicating they are less effective at detecting DD-related changes in ventral hippocampal activity (Supplementary Fig. 4). Fos and Arc also did not differ between WT and TK rats. These results collectively indicate that neurogenesis promotes activity in the ventral hippocampus during delay-based decision-making and that DD-specific activity is best captured by the IEG Zif268.

Delay-based decision-making induces morphological plasticity in adult-born neurons

Structural changes in neuronal morphology are believed to underlie memory and adaptive behavioral changes [50]. We therefore hypothesized that delay-based decision-making would induce plastic changes in adult-born neurons.

To test this, we labeled adult-born neurons with an eGFP-expressing retrovirus and examined neuronal morphology after rats performed the standard DD task or the No Delay (ND) control task that was identical except that rats did not have to wait to receive the high reward (Fig. 4). Since adult-born neurons can undergo experience-dependent morphological plasticity depending on their stage of maturation [51, 52] we examined 2 different-aged populations of neurons. Rats received retrovirus injections at 7 weeks prior to training to label the oldest, most mature, cohort of neurons (“mature”) that were depleted in the TK experiment (Fig. 1), and 3 weeks prior to DD training to label neurons that would be young and highly-plastic at the time of training onset (“immature”). As expected, rats run in the ND task nearly exclusively preferred the high reward in all blocks, whereas rats run in the DD task preferred the high reward less across blocks, i.e., with increasing delay times (group \times block RM ANOVA: effect of group, $F_{3,25} = 47$, $P < 0.0001$; effect of block, $F_{3,75} = 52$, $P < 0.0001$; interaction, $F_{9,75} = 18$, $P < 0.0001$; $n = 6\text{--}8/\text{group}$). Time of surgery did not affect behavior (post hoc Holm-Sidak tests: overall and within-block differences between ND groups all $P > 0.9$ and between DD groups all $P > 0.08$).

Consistent with a role in promoting choice of delayed rewards, dendritic complexity of mature adult-born neurons was selectively increased by DD training, as measured by Sholl analyses, in both the dorsal and ventral DG (Fig. 4G,H). Mature neurons in DD-trained rats also had more branch points and greater total dendritic length than neurons in the ND-trained control group, indicating that learning about delayed rewards specifically recruits and promotes the growth of adult-born neurons (Fig. 4I,J). DD-induced dendritic plasticity was specific to mature neurons, since no effects were observed in immature adult-born neurons (Fig. 4C–F).

To determine whether DD training altered putative synaptic integration of adult-born neurons, we quantified dendritic spines in the molecular layer, where the perforant path terminates onto newborn DG neurons (Fig. 5). We did not observe any effects of DD training on total spine density in immature neurons (Fig. 5B). However, DD training redistributed immature neuron mushroom spines along the dorsoventral axis (Fig. 5C). Whereas neurons in ND-trained rats had similar numbers of mushroom spines in the dorsal and ventral DG, neurons in DD-trained rats had more mushroom spines in the ventral DG than in the dorsal DG. That mushroom spines were reduced in the dorsal DG of DD-trained rats as compared to controls suggests that DD training may in fact reduce or delay the integration of new neurons in this subregion. DD-induced spine plasticity was specific to immature adult-born neurons as no differences were observed in mature adult-born neurons (Fig. 5D, E).

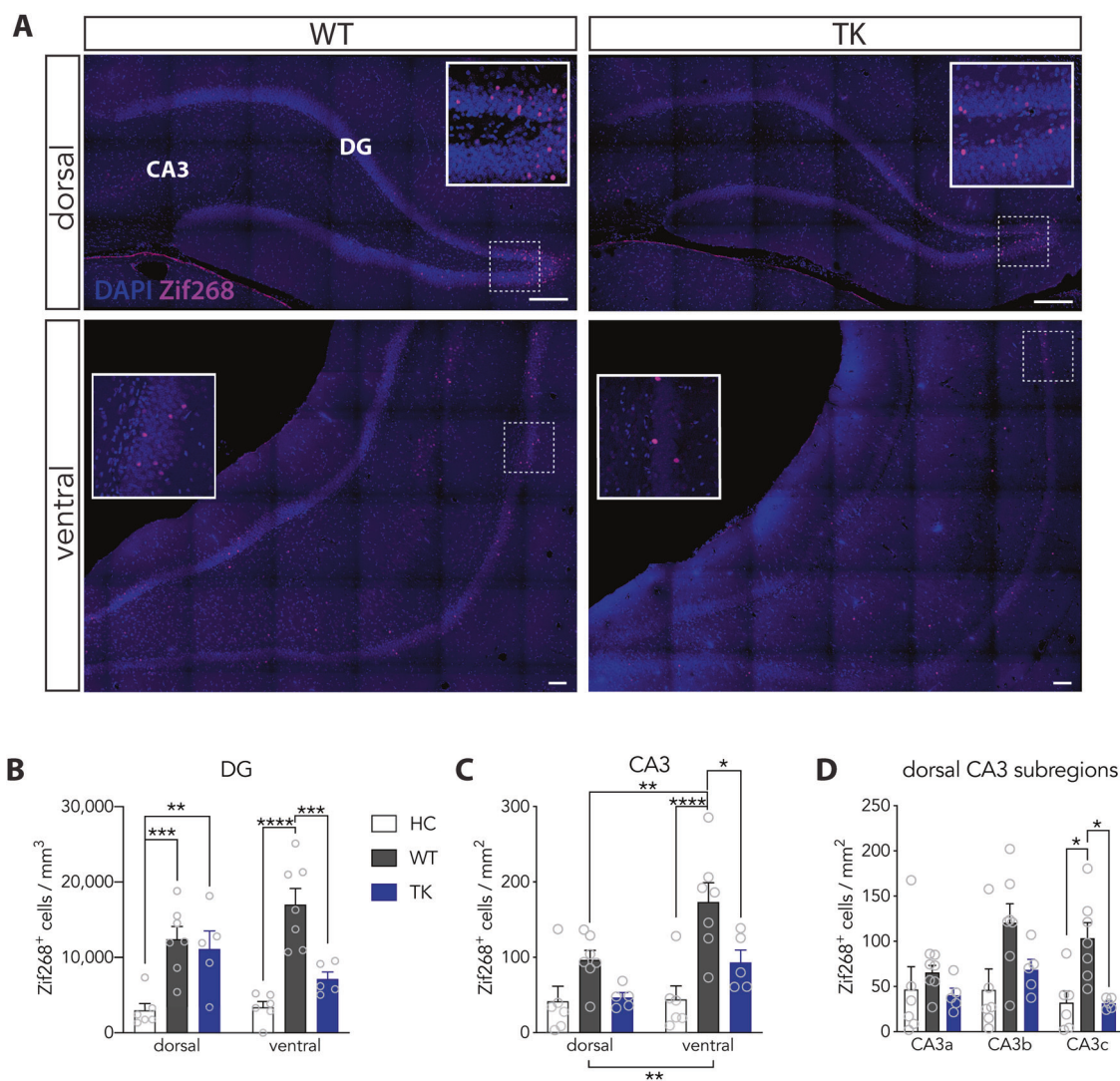


Fig. 3 Loss of neurogenesis decreases Zif268-related activity in the ventral hippocampus. **A** Representative images of Zif268 immunostaining in WT and TK rats in the dorsal and ventral hippocampus 35 min after the last day of performing the DD task. Scale bars: 200 μm. **B** Performing the DD task increased expression of Zif268 in the dorsal DG in both WT and TK rats but only increased Zif268 expression in the ventral DG in neurogenesis-intact WT rats (RM ANOVA; effect of group $F_{2,15} = 20$, $P < 0.0001$; dorsoventral effect $F_{1,15} = 0.1$, $P = 0.8$; interaction effect $F_{2,15} = 5.1$, $P = 0.02$; post-hoc Holm-Sidak tests: dorsal HC vs. dorsal WT, $P = 0.006$; dorsal HC vs. dorsal TK, $P = 0.004$; dorsal WT vs. dorsal TK, $P = 0.6$; ventral HC vs. ventral WT, $P < 0.0001$; ventral HC vs. ventral TK, $P = 0.13$; ventral WT vs. ventral TK, $P = 0.0004$; $n = 5-7$ /group). **C** Performing

the DD task did not alter Zif268⁺ cell densities in dorsal CA3 but increased activity in ventral CA3, specifically in neurogenesis-intact WT rats (ANOVA group effect $F_{2,15} = 10$, $P = 0.0017$; dorsoventral effect $F_{1,15} = 13$, $P = 0.0028$; interaction $F_{2,15} = 3.7$, $P = 0.049$; group differences within dorsal CA3 all $P > 0.1$, ventral HC vs. WT $P < 0.0001$, ventral WT vs. TK $P = 0.01$, HC CO vs. TK $P = 0.08$; $n = 5-7$ /group). **D** Within dorsal CA3, DD training specifically elevated Zif268 expression in CA3c in WT but not TK rats. (RM ANOVA: group effect, $F_{2,15} = 5$, $P = 0.03$; subregion effect, $F_{2,30} = 6$, $P = 0.007$; interaction, $F_{4,30} = 3$, $P = 0.04$). Bars indicate mean \pm standard error. DG dentate gyrus, HC non-transgenic home cage control rats. * $P < 0.05$; ** $P < 0.01$; *** $P < 0.001$; **** $P < 0.0001$.

Delayed reward choice behavior activates adult-born neurons in the ventral DG

Greater mushroom spine density in the ventral DG suggests that these neurons may be specifically recruited during delay-based decision making. To test this, we labeled adult-born neurons with BrdU and quantified IEG expression as rats performed the standard DD task or the ND control task,

described above (Fig. 6). As in the retrovirus experiments, we examined cohorts of adult-born neurons that were immature and mature at the time of testing onset. We also examined superficially-located DAPI⁺ cells to determine activity in putative-developmentally-born DG neurons [42]. Irrespective of the task, mature adult-born neurons were active at higher rates than both immature neurons and the DAPI⁺ population, an effect that was greatest for Zif268

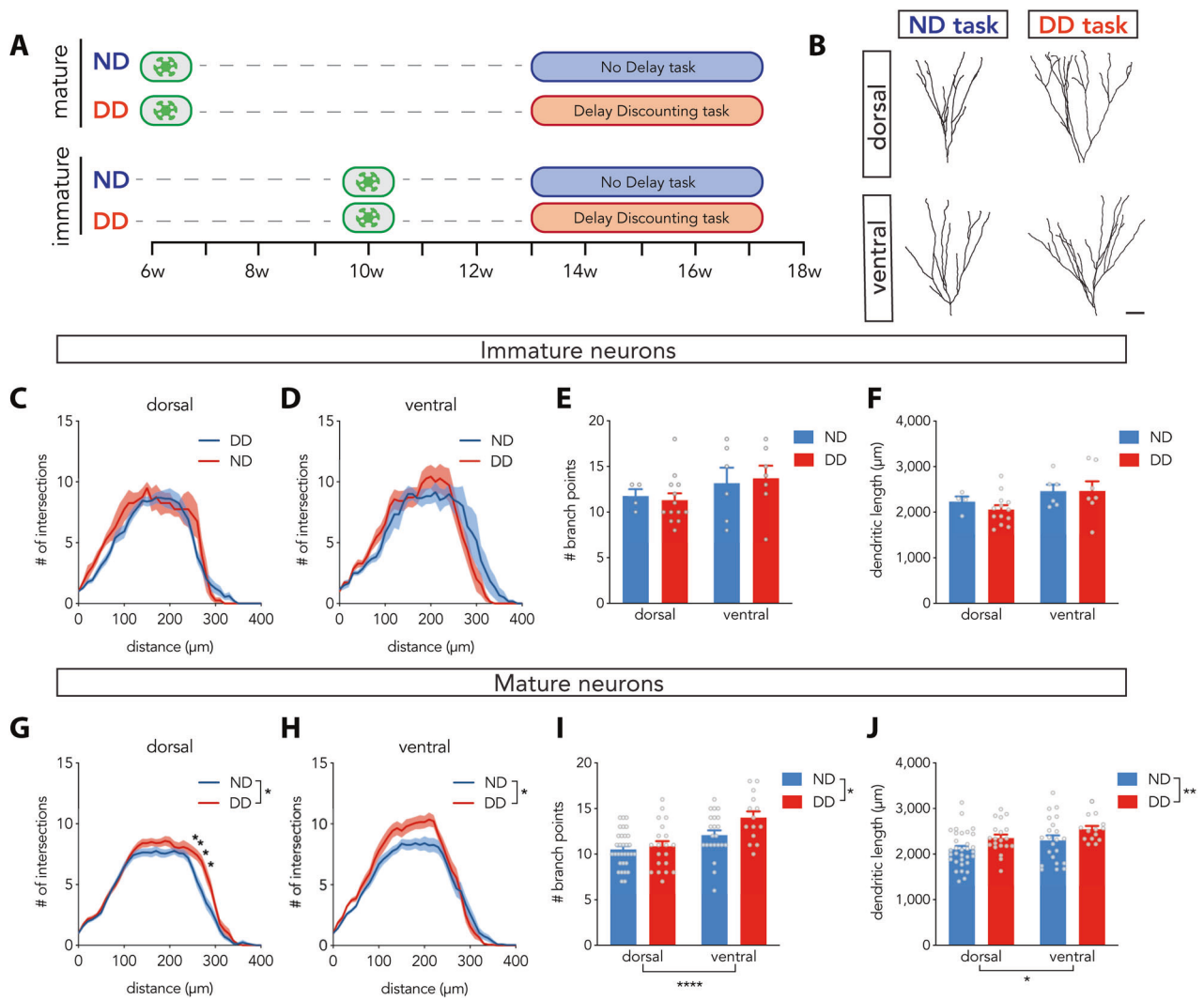


Fig. 4 Delay-based decision-making increases dendritic complexity in new neurons. **A** Experimental timeline: rats were injected with retrovirus either 7 weeks or 3 weeks before training to label cohorts of adult-born neurons that were mature or immature at the time of training onset, respectively. Virus-injected rats were either trained in a no-delay version of the task (ND) or were trained in the standard delay discounting (DD) task. **B** Representative traces of mature adult-born neurons (12-week-old at the end of the experiment) in the dorsal and ventral DG of rats run in the ND and DD tasks. Scale bar, 50 μm . **C** Immature neuron morphology in the dorsal hippocampus was not affected by learning the DD task, as measured by Sholl analyses (RM ANOVA: effect of group, $F_{1,15} = 1.3$, $P = 0.3$, effect of radial distance, $F_{40,600} = 57$, $P < 0.0001$, interaction: $F_{40,600} = 0.92$, $P = 0.6$; $n = 4-13/\text{group}$). **D** Immature neuron morphology in the ventral hippocampus was not affected by learning the DD task (RM ANOVA: effect of group, $F_{1,11} = 0.004$, $P = 0.95$; effect of radial distance, $F_{40,440} = 42.1$, $P < 0.0001$; interaction, $F_{40,440} = 1.5$, $P = 0.03$; $n = 6-7/\text{group}$). **E** Immature neurons had a similar number of dendritic branch points, regardless of task (ANOVA: effect of group, $F_{1,26} = 0.3$, $P = 0.6$; effect of DG region, $F_{1,26} = 4.1$, $P = 0.05$; interaction, $F_{1,26} = 0.3$, $P = 0.6$; $n = 4-13/\text{group}$). **F** Immature neurons had a similar total dendritic length, regardless of task (group x DG region

ANOVA: effect of group, $F_{1,26} = 0.002$, $P = 0.97$, effect of DG region, $F_{1,26} = 2.30$, $P = 0.14$; interaction, $F_{1,26} = 0.15$, $P = 0.70$, $n = 4-13/\text{group}$). **G** Sholl analysis of mature adult-born neurons revealed increased dendritic complexity in the dorsal DG of DD rats compared to ND rats (RM ANOVA: effect of group, $F_{1,49} = 6.0$, $P = 0.017$; effect of radial distance, $F_{41,2009} = 201$, $P < 0.0001$; interaction, $F_{41,2009} = 2.3$, $P < 0.0001$; post-hoc Holm Sidak test: ND vs. DD at 260–290 μm all $P < 0.01$). **H** Sholl analysis of mature adult-born neurons revealed increased dendritic complexity in the ventral DG of DD rats compared to ND rats (effect of group, $F_{1,34} = 4.4$, $P = 0.04$; effect of radial distance, $F_{41,1394} = 137$, $P < 0.0001$, interaction, $F_{41,1394} = 2.0$, $P = 0.0002$; post-hoc Holm Sidak test: ND vs. DD at all radial distances $P > 0.5$; $n = 14-31/\text{group}$). **I** Training on the DD task increased the number of dendritic branch points in mature adult-born neurons (ANOVA: effect of dorsoventral subregion, $F_{1,84} = 20$, $P < 0.0001$; effect of task, $F_{1,84} = 4.5$, $P = 0.04$; interaction, $F_{1,84} = 2.3$, $P = 0.13$; $n = 14-31/\text{group}$). **J** Training on the DD task increased the dendritic length of mature adult-born neurons (ANOVA: effect of dorsoventral subregion, $F_{1,84} = 4.8$, $P = 0.03$; effect of task, $F_{1,84} = 7.6$, $P = 0.007$; interaction, $F_{1,84} = 0.0$, $P = 0.99$; $n = 14-31/\text{group}$). Bars indicate mean \pm standard error. * $P < 0.05$; ** $P < 0.01$.

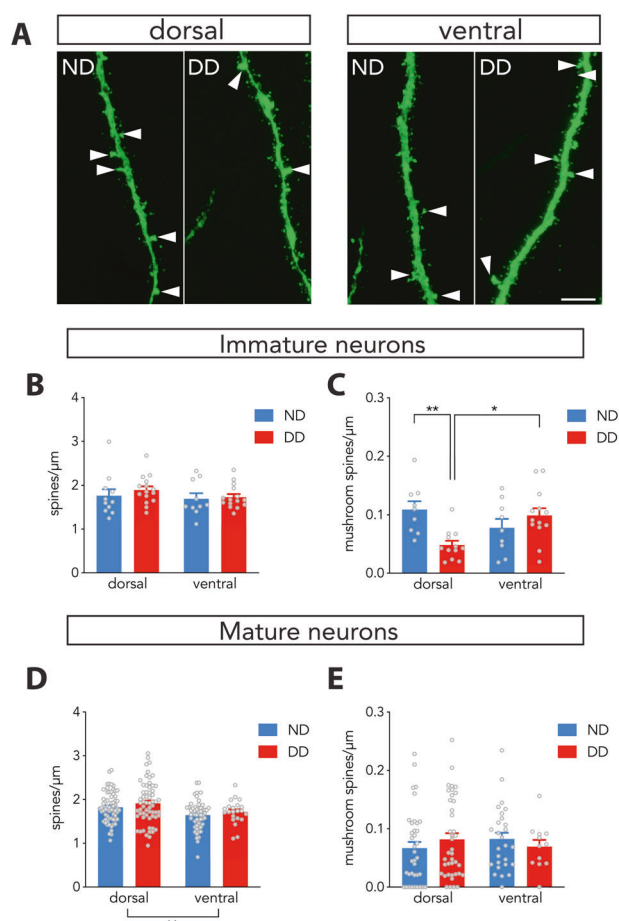


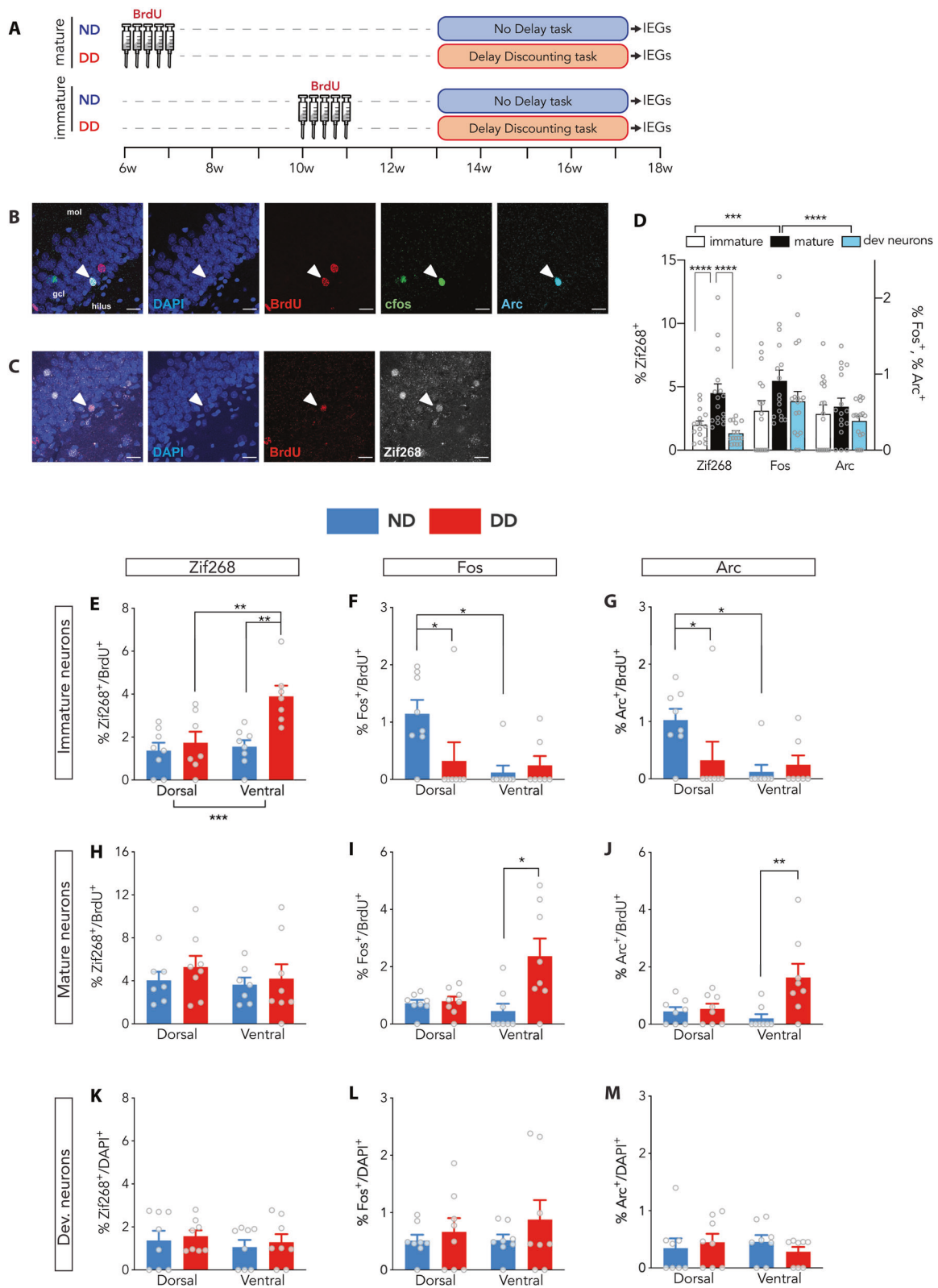
Fig. 5 Delay-based decision-making restructures spines along the dorsoventral axis. **A** Dendritic segments from immature adult-born neurons (8-week-old at the end of the experiment) in the dorsal and the ventral DG. Arrows indicate mushroom spines. Scale bar, 5 μm **B** Learning the DD task did not alter total spine density in immature neurons (ANOVA: effect of group, $F_{1,47} = 0.7$, $P = 0.4$; effect of DG region, $F_{1,47} = 1.2$, $P = 0.3$; interaction, $F_{1,47} = 0.2$, $P = 0.7$; $n = 10\text{--}15/\text{group}$). **C** Whereas mushroom spine density was similar in the dorsal and ventral DG in ND rats, DD training shifted mushroom spine density along the dorsoventral axis, such that dorsal immature neurons had fewer mushroom spines than ventral neurons, and dorsal neurons from DD rats had fewer mushroom spines than dorsal neurons from ND rats (ANOVA; effect of task, $F_{1,39} = 2.6$, $P = 0.11$; effect of dorsoventral subregion, $F_{1,39} = 0.6$, $P = 0.4$; interaction, $F_{1,39} = 11$, $P = 0.002$; dorsal DD vs. dorsal ND $P = 0.008$; dorsal DD vs. ventral DD $P = 0.01$; $n = 9\text{--}13/\text{group}$). **D** Mature adult-born neurons have more total spines in the dorsal DG than in the ventral DG (ANOVA: effect of group, $F_{1,197} = 2.0$, $P = 0.2$; effect of DG region, $F_{1,197} = 10.2$, $P = 0.002$; interaction, $F_{1,197} = 0.02$, $P = 0.9$; $n = 22\text{--}64/\text{group}$). **E** Learning the DD task did not alter the number of mushroom spines on mature neurons (ANOVA: effect of group, $F_{1,1912} = 0.0$, $P = 0.95$; effect of DG region, $F_{1,112} = 0.02$, $P = 0.9$; interaction: $F_{1,12} = 1.2$, $P = 0.3$; $n = 27\text{--}40/\text{group}$). Bars indicate mean \pm standard error. * $P < 0.05$; ** $P < 0.01$.

(Fig. 6D). We also observed distinct patterns of neuronal activity that depended on the task, cell age and IEG activity marker. Notably, DD-trained rats consistently showed specific and preferential recruitment of adult-born neurons in

the ventral DG as compared to ND-trained rats: ventral neurons that were immature at the time of testing were more likely to express Zif268 and ventral neurons that were mature at the time of testing were more likely to express Fos and Arc (Fig. 6E–J). In addition to DD-specific patterns of activation, we also observed evidence for specific recruitment by ND training: within the dorsal DG, immature neurons were more likely to be recruited in ND-trained rats than in DD-trained rats, as measured by Fos and Arc. In contrast to the task-specific patterns of activation within the adult-born population, activity in the putative developmentally-born population of DG neurons was equivalent in ND- and DD-trained rats. These results collectively indicate that adult-born neurons are uniquely and differentially recruited along the dorsoventral axis according to task demands. Whereas new neurons in the dorsal DG are recruited as rats choose between immediately-available rewards, new neurons in the ventral DG are recruited when rats decide between immediate vs. delayed rewards.

Discussion

Here we report that adult-born neurons in rats promote the choice of delayed, larger rewards in an operant decision-making task. Behavioral changes were specifically due to loss of newborn neurons because higher rates of delay discounting were also observed in a radiological model of reduced neurogenesis, and no deficits were observed in intact transgenic rats that were not treated with valganciclovir. Whereas acute stress modulates anxiety and depression-related behaviors in a neurogenesis-dependent fashion [6], we did not observe a stress-dependent role for neurogenesis in the DD task. However, since neurogenesis regulates responding to chronic stressors [47, 53], it may be that neurogenesis-deficient animals' delayed reward preferences are more susceptible to chronic stress. Notably, new neurons are needed to associate events over time [54–57], and so it could be argued that the delay discounting deficit reflects impaired learning about the temporally-discontinuous relationship between the high reward lever choice and reward. This explanation seems unlikely, however, since TK and IR rats clearly preferred the high reward lever in the absence of delay, indicating intact knowledge about the relative value of the two options. Several of our results implicate ventral newborn neurons in delayed reward choice. First, blocking neurogenesis severely blunted task-related IEG activity in the ventral, but not dorsal, DG and CA3. Second, delay-based decision making restructured spines along the dorsoventral axis, such that adult-born neurons in the ventral DG had more mushroom spines than their dorsal counterparts. Third, delay-based decision making specifically activated adult-born neurons in the



ventral DG relative to a control task where rats chose between immediately-available rewards. Given that impulsive decision making is pervasive in psychiatric disorders

[15, 16] our findings identify a specific behavioral function for adult neurogenesis that has broad implications for mental health.

◀ Fig. 6 Specific recruitment of adult-born neurons during delay-based decision making. **A** Experimental design for measuring activity in immature and mature neurons as rats perform the DD and ND tasks. **B** Confocal images of an adult-born BrdU⁺ cell expressing Fos and Arc (mature group, 12 weeks old at the end of the experiment). **C** Confocal images of an adult-born neuron expressing Zif268 (immature group, 8 weeks old at the end of the experiment). Scale bars, 20 μm. **D** During behavioral testing (ND and DD animals pooled), mature adult-born neurons were recruited at higher rates than immature adult-born neurons and the putative developmentally-born neuronal population, specifically for Zif268 (effect of cell population, $F_{2,132} = 15$, $P < 0.0001$, cell population \times IEG interaction, $F_{4,132} = 9.5$, $P < 0.0001$; post hoc Holm Sidak tests: mature vs. immature and overall populations both $P \leq 0.0001$; Zif268 expression in mature vs. immature and overall populations both $P < 0.0001$; Fos and Arc expression comparisons across cell populations all $P > 0.7$; $n = 7$ – 8 /group). **E–M** IEG expression in DG neuronal populations. **E** Immature neurons were more likely to express Zif268 in the ventral hippocampus during the DD task (RM ANOVA: effect of task, $F_{1,13} = 6.5$, $P = 0.003$; effect of dorsoventral subregion, $F_{1,13} = 20.2$, $P = 0.0006$, interaction, $F_{1,13} = 14.4$, $P = 0.002$; post hoc Holm Sidak tests: ventral DD vs. ventral ND, $P = 0.001$; ventral DD vs. dorsal DD $P = 0.0002$; $n = 7$ – 8 /group). **F** Immature neurons were more likely to express Fos in the dorsal hippocampus during the ND task (RM ANOVA: subregion \times task interaction, $F_{1,13} = 5.0$, $P = 0.04$; Kruskal Wallis test $P = 0.009$; post hoc Dunn's test: dorsal ND vs. ventral ND and dorsal DD both $P < 0.05$; $n = 8$ /group). **G** Immature neurons were more likely to express Arc in the dorsal hippocampus during the ND task (RM ANOVA: subregion \times task interaction, $F_{1,13} = 4.6$, $P = 0.05$; Kruskal Wallis test: $P = 0.01$; Post hoc Dunn's test: dorsal ND vs. ventral ND, $P = 0.01$, dorsal ND vs. dorsal DD, $P = 0.07$; $n = 8$ /group). **H** Mature neurons did not display any task specific expression of Zif268 (RM ANOVA: effect of task, $F_{1,13} = 0.5$, $P = 0.5$; effect of subregion, $F_{1,13} = 2.3$, $P = 0.15$; interaction, $F_{1,13} = 0.4$, $P = 0.5$; $n = 8$ /group). **I** Mature neurons in the ventral hippocampus were more likely to express Fos in DD rats than in ND rats (RM ANOVA: task \times subregion interaction, $F_{1,14} = 7.4$, $P = 0.01$; Kruskal Wallis test: $P = 0.01$, Post hoc Dunn's test: DD ventral vs. ND ventral $P = 0.006$; $n = 8$ /group). **J** Mature neurons in the ventral hippocampus were more likely to express Arc in DD rats than in ND rats (RM ANOVA: task \times subregion interaction, $F_{1,14} = 6.2$, $P = 0.02$; Kruskal Wallis test: $P = 0.01$, Post hoc Dunn's test: DD ventral vs. ND ventral $P = 0.005$; $n = 8$ /group). **K–M** The superficial DAPI⁺, putative developmentally-born, population of DG neurons was not differentially recruited during DD testing (for all IEGs, all main effects and interactions $P > 0.3$; $n = 8$ /group). mol, molecular layer, gcl, granule cell layer. Bars indicate mean \pm standard error. * $P < 0.05$, ** $P < 0.01$, *** $P < 0.001$, **** $P < 0.0001$.

Neurogenic and hippocampal functions in delayed reward choice

While the hippocampus is commonly understood in terms of its role in memory for the past, particularly episodic memory, one of the primary functions of memory is to promote adaptive future behavior [58, 59]. Indeed, a common 'core' network, which includes the hippocampus, is recruited during the construction of both past and possible future events [60] and damage to the medial temporal lobe produces profound deficits in re-experiencing of past experiences and "pre-experiencing" possible future events with episodic detail [26]. Furthermore, electrophysiological

recordings confirm that hippocampal neurons process information that is relevant for choices about the future: place cell firing patterns are modulated by goals [61] and reflect future choices in navigational [19, 20, 22, 62] and delay discounting [63] tasks. Indeed, in both humans [27, 28] and rodents [29–31], damage to the hippocampus leads to impulsive decision making in delay discounting tasks. Accordingly, it is intuitive that adult hippocampal neurogenesis would regulate future-oriented decision making. To our knowledge, our findings are the first to identify a specific subpopulation of hippocampal neurons that is critical for preferring future rewards. One recent study found that a subset of DG neurons display reward-specific firing and trigger future-oriented spatial signals in downstream CA3 [21]. While the identity of these cells was not confirmed, our work suggests that adult-born neurons may play such a role, since they were uniquely activated by decisions involving future rewards.

Our observation that neurogenesis-related changes were primarily observed in the ventral hippocampus aligns with theories about functional differentiation along the dorsoventral axis. Much work on the role of the hippocampus in future-oriented choice comes from human studies, which implicate the anterior hippocampus (homolog of the rodent ventral hippocampus) in scene construction functions that could support episodic representation of future experiences [64]. Evidence from humans and rodents indicates that ventral/anterior hippocampal representations tend to be coarse [65, 66], and may therefore provide gist-like contextual information [67–69] that could serve as a scaffold for guiding choices about immediate vs. future rewards. For example, ventral hippocampal neurons display a generalized context signal [70] and are necessary for rats to use contextual information to choose the correct cue to receive a reward [71]. Possibly, in the DD task, adult-born neurons perform a related function and enable rats to envision the immediate context that will result from choice of the small reward lever and the future context that will result from choice of the large reward lever, thereby improving discrimination and encouraging choice of the larger reward. Such a function would be consistent with new neuron functions in context discrimination [72, 73], and evidence that they promote context-specific ensemble codes in CA3 [74]. Given direct anatomical connectivity, the ventral hippocampus is ideally situated to communicate temporal context signals to the prefrontal cortex, which may then interact with the dorsal hippocampus to "fill in the details" about these two possible experiences and guide a decision [67, 75]. Finally, ventral hippocampal signals related to context and reward may also support delayed reward choice via interactions with the nucleus accumbens [76], given the critical role of the accumbens in weighing costs and benefits associated with competing choices [77].

Recent work questions whether adult-born neurons influence behavior directly via enhanced excitability and plasticity, or indirectly via effects on other cell populations [78]. While it is unlikely that these 2 possibilities are entirely exclusive of one another, our immediate-early gene experiment in TK rats clearly indicates that blocking neurogenesis alters activity in non-neurogenic DG-CA3 populations. Our finding that TK rats had reduced activity fits with some previous observations from neurogenesis-deficient animals [79] but conflicts with other studies that found elevated activity [47, 80, 81]. The direction of this modulatory effect may depend on the amount of activity in adult-born neurons, where low vs. high levels of activity lead to inhibition vs. excitation of other DG neurons through monosynaptic connections [82]. For example, medial perforant path inputs may highly activate adult-born neurons which, in turn, excite other granule neurons [82]. Thus, when neurogenesis is disrupted, the hippocampus becomes disengaged during delayed reward choice. While the medial entorhinal cortex has yet to be implicated in DD behavior, its involvement is plausible given that it provides the hippocampus with contextual information that could be critical for envisioning immediate vs. delayed outcomes [83]. It remains unclear why we only observed reduced activity in the ventral DG, but this could result from differential innervation from the entorhinal cortex [84] or other regions including prefrontal, amygdalar or hypothalamic areas [85].

Differential recruitment of DG neurons by reward-based decision-making

Adult-born neurons mature in a systematic fashion, and possess a high level of structural and physiological plasticity during an immature critical period [86]. In particular, cells that are ~4 weeks old display greater long-term potentiation [87] and may be particularly critical for hippocampal memory retrieval [88]. We therefore hypothesized that rats might rely on the plasticity afforded by these cells to generate adaptive responses in the DD task. On the other hand, we reasoned that more mature neurons may also play an important role, given that they receive stronger cortical inputs [89] and yet still possess significant potential for plasticity [90, 91].

Delay-based decision making induced specific patterns of morphological plasticity depending on the age of the cell. Mushroom spine plasticity was selective for ventral immature neurons that were 3–8 weeks-old during DD training, which is when neurons undergo the highest rates of spineogenesis (10x spine and 14x mushroom spine increase from 2 to 7 weeks of cell age [91]). Conversely, dendritic growth was observed in mature neurons that were 7–12 weeks-old during training, which is when adult-born

neurons undergo a later wave of dendritic development [91]. That dendritic growth occurred well beyond the traditional critical window indicates that new neurons possess a long-term reserve of structural plasticity that may be harnessed to optimize reward behaviors, similar to what has been described for spatial learning-induced plasticity [90].

The results of our IEG-activity mapping experiment provide convergent evidence that adult-born neurons in the ventral dentate gyrus are preferentially recruited by the DD task, but suggests that there may be functional differences that depend on cell age. Compared to animals that chose between immediately-available rewards, immature adult-born neurons in the ventral hippocampus upregulated Zif268 expression when rats were given the delayed option. In contrast, mature adult-born neurons selectively increased Fos and Arc expression. This pattern mirrors findings that immature adult-born neurons (3w-old) rely on Zif268 for maturation [92] and can express it at high levels [93], but tend to express Fos and Arc at older ages [94] (6w). However, this cannot fully explain our results because, by the end of the experiment, immature neurons were 6⁺ weeks-old and therefore fully capable of expressing IEGs. One intriguing possibility is that, since different IEGs can tag functionally-distinct ensembles of DG neurons [95], immature and mature cohorts of adult-born neurons are contributing to distinct processes during delay-based decision-making.

In addition to the relatively nuanced differences between immature and mature neurons, we observed more fundamental differences between neurons born at different stages of life. Whereas dorsoventral activity patterns in adult-born neurons differentiated between the ND and DD tasks, superficially-located, and therefore likely developmentally-born [42], neurons were equally recruited. This suggests that adult-born neurons may have a privileged role in delay-based decision making and it adds to a growing body of evidence that DG neurons born at different stages of life have distinct functional properties [91, 96–99] (reviewed in [100]).

In contrast to the ventral activation of newborn neurons in the DD task, our data also points to a potential role for dorsal neurogenesis in reward processing. In particular, immature neurons in the dorsal DG were preferentially activated by the ND task, where rats simply had to choose between small and large immediate rewards. In contrast to proposed roles for the ventral/anterior hippocampus in future event construction, activity in the dorsal/posterior hippocampus is often associated with elaboration of episodic details and immediate perceptual processes [64]. While neither neurogenesis (here and previous reports [12, 101]) nor the hippocampus [102] is required for simple reward discrimination, this suggests that immature neurons in the dorsal hippocampus are particularly sensitive to details and/or choices about immediately-available rewards. Such a role could enhance learning about immediately-available uncertain rewards [14] and it could

regulate motivation to obtain both natural rewards [12] and drugs of abuse [3, 4].

Collectively, these data point to potentially complementary roles for adult-born neurons in different types of reward behavior. While our data primarily implicate ventral neurogenesis in delay-based decision making, we did observe reduced Zif268 expression in dorsal CA3c of TK rats. Thus, neurogenesis may also regulate DD behavior via dorsal CA3 networks, which would be consistent with evidence that the dorsal hippocampus also promotes choice of delayed rewards [102]. It will therefore be important for future studies to investigate how different cohorts of neurons, born at different stages of life, work in concert to support future-oriented choices.

Future reward preference as a trans-disease function for neurogenesis

The list of psychiatric disorders that may be impacted by neurogenesis spans mood disorders [103], schizophrenia [104], addiction [105, 106] and Alzheimer's disease [107]. A major challenge has been to identify how neurogenesis can contribute to such a diverse range of disorders [1]. Since most psychiatric disorders involve disruptions to a variety of circuits, it is clear that hippocampal neurogenesis cannot account for the full range of symptoms of any single disorder. Our approach to this problem was inspired by the NIMH Research Domain Criteria project (RDoC) [2], which aims to identify the neural basis of specific behavioral processes that are disrupted in, and across, traditionally-defined psychiatric disorders. Indeed, delay discounting is a construct within RDoC [108], and it is dysregulated in many conditions that are associated with neurogenesis impairments, including aging [109], schizophrenia [110], addiction [111], and depression [112]. Thus, by using a translationally-relevant task, we found that neurogenesis directly regulates a reward behavior that goes awry in a substantial segment of the population. Since strategies that recruit the hippocampus promote choice of advantageous delayed rewards [23, 28], our data identify neurogenesis as a potential therapeutic target for reducing impulsive choice and fostering better decisions.

Data availability

The datasets generated during and/or analyzed during the current study are available from the corresponding author upon request.

Acknowledgements This work was supported by the Canadian Institutes of Health Research (JSS, SBF), the Michael Smith Foundation for Health Research (JSS), a NARSAD Young Investigator Grant from the Brain & Behavior Research Foundation (DRS) and the German Research Foundation (DRS). We thank Daniela Palombo for valuable feedback and discussion.

Compliance with ethical standards

Conflict of interest The authors declare no competing interests.

Publisher's note Springer Nature remains neutral with regard to jurisdictional claims in published maps and institutional affiliations.

References

1. Yun S, Reynolds RP, Masiulis I, Eisch AJ. Re-evaluating the link between neuropsychiatric disorders and dysregulated adult neurogenesis. *Nat Publ Group*. 2016;22:1239–47.
2. Cuthbert BN, Insel TR. Toward the future of psychiatric diagnosis: the seven pillars of RDoC. *BMC Med*. 2013;11:126.
3. Noonan MA, Bulin SE, Fuller DC, Eisch AJ. Reduction of adult hippocampal neurogenesis confers vulnerability in an animal model of cocaine addiction. *J Neurosci*. 2010;30:304–15.
4. Deroche-Gamonet V, Revest J-M, Fiancette J-F, Balado E, Koehl M, Grosjean N, et al. Depleting adult dentate gyrus neurogenesis increases cocaine-seeking behavior. *Mol Psychiatry*. 2018;229:1.
5. Galinato MH, Takashima Y, Fannon MJ, Quach LW, Silva RJM, Mysore KK, et al. Neurogenesis during abstinence is necessary for context-driven methamphetamine-related memory. *J Neurosci*. 2018;38:2011. 17–14
6. Snyder JS, Soumier A, Brewer M, Pickel J, Cameron HA. Adult hippocampal neurogenesis buffers stress responses and depressive behaviour. *Nature*. 2011;476:458–61.
7. Snyder JS, Grigereit L, Russo A, Seib DR, Brewer M, Pickel J, et al. A transgenic rat for specifically inhibiting adult neurogenesis. *Eneuro*. 2016;3:e0064–16. 1–13
8. Seib DRM, Corsini NS, Ellwanger K, Plaas C, Mateos A, Pitzer C, et al. Loss of dickkopf-1 restores neurogenesis in old age and counteracts cognitive decline. *Cell Stem Cell*. 2013;12:204–14.
9. Bessa JM, Ferreira D, Melo I, Marques F, Cerqueira JJ, Palha JA, et al. The mood-improving actions of antidepressants do not depend on neurogenesis but are associated with neuronal remodeling. *Mol Psychiatry*. 2009;14:764. 73–739
10. Schoenfeld TJ, McCausland HC, Morris HD, Padmanaban V, Cameron HA. Stress and loss of adult neurogenesis differentially reduce hippocampal volume. *Biol Psychiatry*. 2017;82:1–34.
11. Egeland M, Guinaudie C, Preez AD, Musaelyan K, Zunszain PA, Fernandes C, et al. Depletion of adult neurogenesis using the chemotherapy drug temozolomide in mice induces behavioural and biological changes relevant to depression. *Transl Psychiat*. 2017;7:e1101–e1101.
12. Karlsson R, Wang AS, Sonti AN, Cameron HA. Adult neurogenesis affects motivation to obtain weak, but not strong, reward in operant tasks. *Hippocampus*. 2018;28:512–22.
13. Treadway MT, Zald DH. Parsing Anhedonia: Translational Models of Reward-Processing Deficits in Psychopathology. *Curr Directions Psychological Sci*. 2013;22:244–9.
14. Seib DR, Espinueva DF, Floresco SB, Snyder JS. A role for neurogenesis in probabilistic reward learning. *Behav Neurosci*. 2020;134:1–13.
15. Bickel WK, Jarmolowicz DP, Mueller ET, Koffarnus MN, Gatchalian KM. Excessive discounting of delayed reinforcers as a trans-disease process contributing to addiction and other disease-related vulnerabilities: emerging evidence. *Pharmacol Therapeutics*. 2012;134:287–97.
16. Volkow ND, Baler RD. NOW vs LATER brain circuits: implications for obesity and addiction. *Trends Neurosci*. 2015;38:345–52.
17. Der-Avakian A, Markou A. The neurobiology of anhedonia and other reward-related deficits. *Trends Neurosci*. 2012;35:68–77.

18. Winstanley CA, Floresco SB. Deciphering decision making: variation in animal models of effort- and uncertainty-based choice reveals distinct neural circuitries underlying core cognitive processes. *J Neurosci: Off J Soc Neurosci*. 2016;36:12069–79.
19. Johnson A, Redish AD. Neural ensembles in CA3 transiently encode paths forward of the animal at a decision point. *J Neurosci*. 2007;27:12176–89.
20. Pfeiffer BE, Foster DJ. Hippocampal place-cell sequences depict future paths to remembered goals. *Nature*. 2013;497:74–9.
21. Sasaki T, Piatti VC, Hwaun E, Ahmadi S, Lisman JE, Leutgeb S, et al. Dentate network activity is necessary for spatial working memory by supporting CA3 sharp-wave ripple generation and prospective firing of CA3 neurons. *Nat Neurosci*. 2018;21:258–69.
22. Kay K, Chung JE, Sosa M, Schor JS, Karlsson MP, Larkin MC, et al. Constant sub-second cycling between representations of possible futures in the hippocampus. *Cell*. 2020;180:1–16.
23. Peters J, Büchel C. Episodic future thinking reduces reward delay discounting through an enhancement of prefrontal-mediocortical interactions. *Neuron*. 2010;66:138–48.
24. Benoit RG, Gilbert SJ, Burgess PW. A neural mechanism mediating the impact of episodic prospection on farsighted decisions. *J Neurosci*. 2011;31:6771–9.
25. Hassabis D, Kumaran D, Vann SD, Maguire EA. Patients with hippocampal amnesia cannot imagine new experiences. *Proc Natl Acad Sci*. 2007;104:1726–31.
26. Race E, Keane MM, Verfaellie M. Medial temporal lobe damage causes deficits in episodic memory and episodic future thinking not attributable to deficits in narrative construction. *J Neurosci*. 2011;31:10262–9.
27. Lebreton M, Bertoux M, Boutet C, Lehericy S, Dubois B, Fossati P, et al. A critical role for the hippocampus in the valuation of imagined outcomes. *PLoS Biol*. 2013;11:e1001684.
28. Palombo DJ, Keane MM, Verfaellie M. The medial temporal lobes are critical for reward-based decision making under conditions that promote episodic future thinking. *Hippocampus*. 2015;25:345–53.
29. Rawlins JN, Feldon J, Butt S. The effects of delaying reward on choice preference in rats with hippocampal or selective septal lesions. *Behavioural Brain Res*. 1985;15:191–203.
30. Cheung TH, Cardinal RN. Hippocampal lesions facilitate instrumental learning with delayed reinforcement but induce impulsive choice in rats. *BMC Neurosci*. 2005;6:36.
31. Abela AR, Chudasama Y. Dissociable contributions of the ventral hippocampus and orbitofrontal cortex to decision-making with a delayed or uncertain outcome. *Eur J Neurosci*. 2013;37:640–7.
32. Yu RQ, Cooke M, Seib DR, Zhao J, Snyder JS. Adult neurogenesis promotes efficient, nonspecific search strategies in a spatial alternation water maze task. *Behav Brain Res*. 2019;376:112151.
33. Seib DR, Chahley E, Princz-Lebel O, Snyder JS. Intact memory for local and distal cues in male and female rats that lack adult neurogenesis. *PLoS One*. 2018;13:e0197869–15.
34. Parent JM, Tada E, Fike JR, Lowenstein DH. Inhibition of dentate granule cell neurogenesis with brain irradiation does not prevent seizure-induced mossy fiber synaptic reorganization in the rat. *J Neurosci*. 1999;19:4508–19.
35. van Praag H, Schinder AF, Christie BR, Toni N, Palmer TD, Gage FH. Functional neurogenesis in the adult hippocampus. *Nature*. 2002;415:1030–4.
36. Seib D, Martin-Villalba A. In vivo neurogenesis. *Bio-Protocol*. 2013;3:1–8.
37. Schindelin J, Arganda-Carreras I, Frise E, Kaynig V, Longair M, Pietzsch T, et al. Fiji: an open-source platform for biological-image analysis. *Nat Methods*. 2012;9:676–82.
38. Longair MH, Baker DA, Armstrong JD. Simple Neurite Tracer: open source software for reconstruction, visualization and analysis of neuronal processes. *Bioinforma*. 2011;27:2453–4.
39. Seib D, Martin-Villalba A. Neuronal morphology analysis. *Bio-Protocol*. 2013;3:1–7.
40. Denny CA, Kheirbek MA, Alba EL, Tanaka KF, Brachman RA, Laughman KB, et al. Hippocampal memory traces are differentially modulated by experience, time, and adult neurogenesis. *Neuron*. 2014;83:189–201.
41. Schlessinger AR, Cowan WM, Gottlieb DI. An autoradiographic study of the time of origin and the pattern of granule cell migration in the dentate gyrus of the rat. *J Comp Neurol*. 1975;159:149–75.
42. Ciric T, Cahill SP, Snyder JS. Dentate gyrus neurons that are born at the peak of development, but not before or after, die in adulthood. *Brain Behav*. 2019;9:e01435.
43. Zeeb FD, Floresco SB, Winstanley CA. Contributions of the orbitofrontal cortex to impulsive choice: interactions with basal levels of impulsivity, dopamine signalling, and reward-related cues. *Psychopharmacology*. 2010;211:87–98.
44. Harrison PJ. The hippocampus in schizophrenia: a review of the neuropathological evidence and its pathophysiological implications. *Psychopharmacology*. 2004;174:151–62.
45. Yassa MA, Stark SM, Bakker A, Albert MS, Gallagher M, Stark CEL. High-resolution structural and functional MRI of hippocampal CA3 and dentate gyrus in patients with amnesic Mild Cognitive Impairment. *Neuroimage*. 2010;51:1242–52.
46. Jack CR, Petersen RC, Xu Y, O'Brien PC, Smith GE, Ivnik RJ, et al. Rates of hippocampal atrophy correlate with change in clinical status in aging and AD. *Neurology*. 2000;55:484–90.
47. Anacker C, Luna VM, Stevens GS, Millette A, Shores R, Jimenez JC, et al. Hippocampal neurogenesis confers stress resilience by inhibiting the ventral dentate gyrus. *Nature*. 2018;559:1–22.
48. Lehmann ML, Brachman RA, Martinowich K, Schloesser RJ, Herkenham M. Glucocorticoids orchestrate divergent effects on mood through adult neurogenesis. *J Neurosci*. 2013;33:2961–72.
49. Shafiei N, Gray M, Viau V, Floresco SB. Acute stress induces selective alterations in cost/benefit decision-making. *Neuropsychopharmacol*. 2012;37:2194–209.
50. Yang G, Pan F, Gan W-B. Stably maintained dendritic spines are associated with lifelong memories. *Nature*. 2009;462:920–4.
51. Alvarez DD, Giacomini D, Yang SM, Trincherro MF, Temprana SG, Büttner KA, et al. A disynaptic feedback network activated by experience promotes the integration of new granule cells. *Science*. 2016;354:459–65.
52. Bergami M, Masserdotti G, Temprana SG, Motori E, Eriksson TM, Göbel J, et al. A critical period for experience-dependent remodeling of adult-born neuron connectivity. *Neuron*. 2015;85:710–7.
53. Schloesser RJ, Lehmann M, Martinowich K, Manji HK, Herkenham M. Environmental enrichment requires adult neurogenesis to facilitate the recovery from psychosocial stress. *Mol Psychiatry*. 2010;15:1152–63.
54. Shors TJ, Miesegae G, Beylin A, Zhao M, Rydel T, Gould E. Neurogenesis in the adult is involved in the formation of trace memories. *Nature*. 2001;410:372–6.
55. Shors TJ, Townsend DA, Zhao M, Kozorovitskiy Y, Gould E. Neurogenesis may relate to some but not all types of hippocampal-dependent learning. *Hippocampus*. 2002;12:578–84.
56. Seo DO, Carillo MA, Lim SC-H, Tanaka KF, Drew MR. Adult Hippocampal Neurogenesis Modulates Fear Learning through Associative and Nonassociative Mechanisms. *J Neurosci*. 2015;35:11330–45.
57. Aimone JB, Wiles J, Gage FH. Potential role for adult neurogenesis in the encoding of time in new memories. *Nat Neurosci*. 2006;9:723–7.
58. Buckner RL. The role of the hippocampus in prediction and imagination. *Annu Rev Psychol*. 2010;61:27–48.
59. Mullally SL, Maguire EA. Memory, imagination, and predicting the future. *Neuroscientist*. 2014;20:220–34.

60. Addis DR, Wong AT, Schacter DL. Remembering the past and imagining the future: common and distinct neural substrates during event construction and elaboration. *Neuropsychologia*. 2007;45:1363–77.
61. Ferbinteanu J, Shapiro ML. Prospective and retrospective memory coding in the hippocampus. *Neuron*. 2003;40:1227–39.
62. Wikenheiser AM, Redish AD. Hippocampal theta sequences reflect current goals. *Nat Neurosci*. 2015;18:289–94.
63. Masuda A, Sano C, Zhang Q, Goto H, McHugh TJ, Fujisawa S, et al. The hippocampus encodes delay and value information during delay-discounting decision making. *Elife*. 2020;9:e52466.
64. Zeidman P, Maguire EA. Anterior hippocampus: the anatomy of perception, imagination and episodic memory. *Nat Rev Neurosci*. 2016;17:173–82.
65. Brunec IK, Bellana B, Ozubko JD, Man V, Robin J, Liu Z-X, et al. Multiple scales of representation along the hippocampal anteroposterior axis in humans. *Curr Biol*. 2018;28:2129–e6.
66. Kjelstrup KB, Solstad T, Brun VH, Hafting T, Leutgeb S, Witter MP, et al. Finite scale of spatial representation in the hippocampus. *Science*. 2008;321:140–3.
67. Eichenbaum H. Prefrontal–hippocampal interactions in episodic memory. *Nat Rev Neurosci*. 2017;18:547–58.
68. Sekeres MJ, Winocur G, Moscovitch M. The hippocampus and related neocortical structures in memory transformation. *Neurosci Lett*. 2018;680:39–53.
69. Sheldon S, Levine B. The role of the hippocampus in memory and mental construction. *Ann NY Acad Sci*. 2016;1369:76–92.
70. Komorowski RW, Garcia CG, Wilson A, Hattori S, Howard MW, Eichenbaum H. Ventral hippocampal neurons are shaped by experience to represent behaviorally relevant contexts. *J Neurosci*. 2013;33:8079–87.
71. Riaz S, Schumacher A, Sivagurunathan S, Meer MVD, Ito R. Ventral, but not dorsal, hippocampus inactivation impairs reward memory expression and retrieval in contexts defined by proximal cues. *Hippocampus*. 2017;27:822–36.
72. Tronel S, Belnoue L, Grosjean N, Revest J-M, Piazza P-V, Koehl M, et al. Adult-born neurons are necessary for extended contextual discrimination. *Hippocampus*. 2012;22:292–8.
73. Sahay A, Scobie KN, Hill AS, O'Carroll CM, Kheirbek MA, Burghardt NS, et al. Increasing adult hippocampal neurogenesis is sufficient to improve pattern separation. *Nature*. 2011;472:466–70.
74. Niibori Y, Yu T-S, Epp JR, Akers KG, Josselyn SA, Frankland PW. Suppression of adult neurogenesis impairs population coding of similar contexts in hippocampal CA3 region. *Nat Commun*. 2012;3:1253.
75. Campbell KL, Madore KP, Benoit RG, Thakral PP, Schacter DL. Increased hippocampus to ventromedial prefrontal connectivity during the construction of episodic future events. *Hippocampus*. 2018;28:76–80.
76. Abela AR, Duan Y, Chudasama Y. Hippocampal interplay with the nucleus accumbens is critical for decisions about time. *Eur J Neurosci*. 2015;42:2224–33.
77. Floresco SB. The nucleus accumbens: an interface between cognition, emotion, and action. *Annual Rev Psychol*. 2014;66:25–52.
78. Park EH, Burghardt NS, Dvorak D, Hen R, Fenton AA. Experience-dependent regulation of dentate gyrus excitability by adult-born granule cells. *J Neurosci*. 2015;35:11656–66.
79. Glover LR, Schoenfeld TJ, Karlsson R-M, Bannerman DM, Cameron HA. Ongoing neurogenesis in the adult dentate gyrus mediates behavioral responses to ambiguous threat cues. *PLoS Biol*. 2017;15:e2001154.
80. Drew LJ, Kheirbek MA, Luna VM, Denny CA, Cloidt MA, Wu MV, et al. Activation of local inhibitory circuits in the dentate gyrus by adult-born neurons. *Hippocampus*. 2015;26:763–78.
81. Burghardt NS, Park EH, Hen R, Fenton AA. Adult-born hippocampal neurons promote cognitive flexibility in mice. *Hippocampus*. 2012;22:1795–808.
82. Luna VM, Anacker C, Burghardt NS, Khandaker H, Andreu V, Millette A, et al. Adult-born hippocampal neurons bidirectionally modulate entorhinal inputs into the dentate gyrus. *Science*. 2019;364:578–83.
83. Knierim JJ, Neunuebel JP, Deshmukh SS. Functional correlates of the lateral and medial entorhinal cortex: objects, path integration and local-global reference frames. *Philos Trans R Soc B*. 2014;369:20130369.
84. Dolorfo CL, Amaral DG. Entorhinal cortex of the rat: topographic organization of the cells of origin of the perforant path projection to the dentate gyrus. *J Comp Neurol*. 1998;398:25–48.
85. Strange BA, Witter MP, Lein ES, Moser EI. Functional organization of the hippocampal longitudinal axis. *Nat Rev Neurosci*. 2014;15:655–69.
86. Jahn HM, Bergami M. Critical periods regulating the circuit integration of adult-born hippocampal neurons. *Cell Tissue Res*. 2018;371:23–32.
87. Ge S, Yang C-H, Hsu K-S, Ming G-L, Song H. A critical period for enhanced synaptic plasticity in newly generated neurons of the adult brain. *Neuron*. 2007;54:559–66.
88. Gu Y, Arruda-Carvalho M, Wang J, Janoschka SR, Josselyn SA, Frankland PW, et al. Optical controlling reveals time-dependent roles for adult-born dentate granule cells. *Nat Neurosci*. 2012;15:1700–6.
89. Dieni CV, Panichi R, Aimone JB, Kuo CT, Wadiche JJ, Wadiche LO. Low excitatory innervation balances high intrinsic excitability of immature dentate neurons. *Nat Commun*. 2016;7:11313.
90. Lemaire V, Tronel S, Montaron M-F, Fabre A, Dugast E, Abrous DN. Long-lasting plasticity of hippocampal adult-born neurons. *J Neurosci*. 2012;32:3101–8.
91. Cole JD, Espinueva D, Seib DR, Ash AM, Cooke MB, Cahill SP, et al. Adult-born hippocampal neurons undergo extended development and are morphologically distinct from neonatally-born neurons prolonged development of adult-born neurons. *J Neurosci*. 2020;40:5740–56.
92. Veyrac A, Gros A, Bruel-Jungerman E, Rochefort C, Borgmann FBK, Jessberger S, et al. Zif268/egr1 gene controls the selection, maturation and functional integration of adult hippocampal newborn neurons by learning. *Proc Natl Acad Sci*. 2013;110:7062–7.
93. Snyder JS, Choe JS, Clifford MA, Jeurling SI, Hurley P, Brown A, et al. Adult-born hippocampal neurons are more numerous, faster maturing, and more involved in behavior in rats than in mice. *J Neurosci*. 2009;29:14484–95.
94. Kee N, Teixeira CM, Wang AH, Frankland PW. Preferential incorporation of adult-generated granule cells into spatial memory networks in the dentate gyrus. *Nat Neurosci*. 2007;10:355–62.
95. Sun X, Bernstein MJ, Meng M, Rao S, Sørensen AT, Yao L, et al. Functionally distinct neuronal ensembles within the memory engram. *Cell*. 2020;181:1–32.
96. Ohline SM, Wake KL, Hawkrigde M-V, Dinnunhan MF, Hegemann RU, Wilson A, et al. Adult-born dentate granule cell excitability depends on the interaction of neuron age, ontogenetic age and experience. *Brain Struct Funct*. 2018;383:335.
97. Tronel S, Lemaire V, Charrier V, Montaron M-F, Abrous DN. Influence of ontogenetic age on the role of dentate granule neurons. *Brain Struct Funct*. 2015;220:645–61.
98. Erwin SR, Sun W, Copeland M, Lindo S, Spruston N, Cembrowski MS. A sparse, spatially biased subtype of mature granule cell dominates recruitment in hippocampal-associated behaviors. *Cell Rep*. 2020;31:107551.

99. Sun D, Milibari L, Pan J-X, Ren X, Yao L-L, Zhao Y, et al. Critical roles of embryonic born dorsal dentate granule neurons for activity-dependent increases in BDNF, adult hippocampal neurogenesis, and antianxiety-like behaviors. *Biol Psychiat* 2021;89:600–14.
100. Snyder JS. Recalibrating the relevance of adult neurogenesis. *Trends Neurosci*. 2019;42:164–78.
101. Swan AA, Clutton JE, Chary PK, Cook SG, Liu GG, Drew MR. Characterization of the role of adult neurogenesis in touch-screen discrimination learning. *Hippocampus*. 2014; 24:1581–91.
102. McHugh SB, Campbell TG, Taylor AM, Rawlins JNP, Bannerman DM. A role for dorsal and ventral hippocampus in inter-temporal choice cost-benefit decision making. *Behav Neurosci*. 2008;122:1–8.
103. Petrik D, Lagace DC, Eisch AJ. The neurogenesis hypothesis of affective and anxiety disorders: are we mistaking the scaffolding for the building? *Neuropharmacology*. 2012;62:21–34.
104. Iannitelli A, Quartini A, Tirassa P, Bersani G. Schizophrenia and neurogenesis: a stem cell approach. *Neurosci Biobehav Rev*. 2017; 80:414–42.
105. Mandyam CD, Koob GF. The addicted brain craves new neurons: putative role for adult-born progenitors in promoting recovery. *Trends Neurosci*. 2012;35:250–60.
106. Chambers RA. Adult hippocampal neurogenesis in the pathogenesis of addiction and dual diagnosis disorders. *Drug Alcohol Depen*. 2012;130:1–12.
107. Moreno-Jiménez EP, Flor-García M, Terreros-Roncal J, Rábano A, Cafini F, Pallas-Bazarra N, et al. Adult hippocampal neurogenesis is abundant in neurologically healthy subjects and drops sharply in patients with Alzheimer’s disease. *Nat Publ Group*. 2019;108:621.
108. Lempert KM, Steinglass JE, Pinto A, Kable JW, Simpson HB. Can delay discounting deliver on the promise of RDoC? *Psychol Med*. 2019;49:190–9.
109. Lempert KM, Mechanic-Hamilton DJ, Xie L, Wisse LEM, Flores R, de, Wang J, et al. Neural and behavioral correlates of episodic memory are associated with temporal discounting in older adults. *Neuropsychologia*. 2020;146:107549.
110. Heerey EA, Robinson BM, McMahon RP, Gold JM. Delay discounting in schizophrenia. *Cogn Neuropsychiatry*. 2007;12:213–21.
111. Madden GJ, Petry NM, Badger GJ, Bickel WK. Impulsive and self-control choices in opioid-dependent patients and non-drug-using control participants: drug and monetary rewards. *Exp Clin Psychopharm*. 1997;5:256–62.
112. Pulcu E, Trotter PD, Thomas EJ, McFarquhar M, Juhasz G, Sahakian BJ, et al. Temporal discounting in major depressive disorder. *Psychological Med*. 2014;44:1825–34.